Acta Biomaterialia 49 (2017) 329–343

Contents lists available at ScienceDirect

Acta Biomaterialia

journal homepage: www.elsevier.com/locate/actabiomat

Full length article

3D culture of human pluripotent stem cells in RGD-alginate hydrogel improves retinal tissue development

Nicola C. Hunt [a], Dean Hallam [a], Ayesha Karimi [c], Carla B. Mellough [a], Jinju Chen [b], David H.W. Steel [a,d], Majlinda Lako [a,*]

[a] Institute of Genetic Medicine, Newcastle University, International Centre for Life, Central Parkway, Newcastle NE1 3BZ, UK
[b] School of Mechanical & Systems Engineering, Stephenson Building, Newcastle University, Newcastle upon Tyne, UK
[c] Cumberland Infirmary, North Cumbria University Hospitals NHS Trust, Carlisle CA2 7HY, UK
[d] Sunderland Eye Infirmary, Queen Alexandra Road, Sunderland SR2 9HP, UK

ARTICLE INFO

Article history:
Received 11 July 2016
Received in revised form 1 November 2016
Accepted 3 November 2016
Available online 5 November 2016

Keywords:
Retina
Tissue engineering
Embryonic stem cells
Induced pluripotent stem cells
Biomaterials

ABSTRACT

No treatments exist to effectively treat many retinal diseases. Retinal pigmented epithelium (RPE) and neural retina can be generated from human embryonic stem cells/induced pluripotent stem cells (hESCs/hiPSCs). The efficacy of current protocols is, however, limited. It was hypothesised that generation of laminated neural retina and/or RPE from hiPSCs/hESCs could be enhanced by three dimensional (3D) culture in hydrogels. hiPSC- and hESC-derived embryoid bodies (EBs) were encapsulated in 0.5% RGD-alginate; 1% RGD-alginate; hyaluronic acid (HA) or HA/gelatin hydrogels and maintained until day 45. Compared with controls (no gel), 0.5% RGD-alginate increased: the percentage of EBs with pigmented RPE foci; the percentage EBs with optic vesicles (OVs) and pigmented RPE simultaneously; the area covered by RPE; frequency of RPE cells (CRALBP+); expression of RPE markers (*TYR* and *RPE65*) and the retinal ganglion cell marker, *MATH5*. Furthermore, 0.5% RGD-alginate hydrogel encapsulation did not adversely affect the expression of other neural retina markers (*PROX1, CRX, RCVRN, AP2α* or *VSX2*) as determined by qRT-PCR, or the percentage of *VSX2* positive cells as determined by flow cytometry. 1% RGD-alginate increased the percentage of EBs with OVs and/or RPE, but did not significantly influence any other measures of retinal differentiation. HA-based hydrogels had no significant effect on retinal tissue development. The results indicated that derivation of retinal tissue from hESCs/hiPSCs can be enhanced by culture in 0.5% RGD-alginate hydrogel. This RGD-alginate scaffold may be useful for derivation, transport and transplantation of neural retina and RPE, and may also enhance formation of other pigmented, neural or epithelial tissue.

Statement of Significance

The burden of retinal disease is ever growing with the increasing age of the world-wide population. Transplantation of retinal tissue derived from human pluripotent stem cells (PSCs) is considered a promising treatment. However, derivation of retinal tissue from PSCs using defined media is a lengthy process and often variable between different cell lines.
This study indicated that alginate hydrogels enhanced retinal tissue development from PSCs, whereas hyaluronic acid-based hydrogels did not. This is the first study to show that 3D culture with a biomaterial scaffold can improve retinal tissue derivation from PSCs.
These findings indicate potential for the clinical application of alginate hydrogels for the derivation and subsequent transplantation retinal tissue. This work may also have implications for the derivation of other pigmented, neural or epithelial tissue.

1. Introduction

In 2010, it was estimated that globally 32.4 million people were classified blind, and 191 million were visually impaired [1]. Diseases affecting the retina account for approximately 26% of

* Corresponding author.
E-mail addresses: nicola.hunt@ncl.ac.uk (N.C. Hunt), dean.hallam@ncl.ac.uk (D. Hallam), carla.mellough@ncl.ac.uk (C.B. Mellough), jinju.chen@ncl.ac.uk (J. Chen), david.steel@ncl.ac.uk (D.H.W. Steel), majlinda.lako@ncl.ac.uk (M. Lako).

http://dx.doi.org/10.1016/j.actbio.2016.11.016
1742-7061/

blindness globally and 70% of blindness in the UK [2]. The burden of retinal disease is ever growing with the increasing age of the world-wide population [3,4]. Both neural retina and the supportive retinal pigmented epithelium (RPE) fail to regenerate in humans, therefore diseases that cause retinal cell loss, such as age-related macular degeneration (AMD), retinitis pigmentosa (RP) and other hereditary retinal dystrophies including glaucoma and vascular retinopathies, typically result in permanent visual impairment [5].

The transplantation of retinal tissue and other cell types has been explored to treat retinal disease. A clinical trial involving 10 patients either with AMD or RP showed that visual acuity was improved in 70% of patients by the transplantation of human foetal neural retina together with RPE into the subretinal space, without the use of immunosuppression [6]. Conversely, the transplantation of adult retinal cells has proved unsuccessful [7,8]. There is, however, limited availability of foetal tissue for transplantation, and the ethical issues associated with this approach mean that it is unlikely to be a feasible treatment option for a large number of patients.

In 2007, it was shown that human induced pluripotent stem cells (hiPSCs) can be generated from patients' dermal fibroblasts [9]. hiPSCs, like embryonic stem cells (hESCs) can be differentiated into both laminated neural retina and RPE [10–14]. Transplantation of retinal cells derived from hESCs and hiPSCs is considered to be a promising treatment for patients with macular degeneration and inherited retinal disease. Shirai et al. [15] were able to show that hESC can be coaxed to differentiate to laminated retinae which upon transplantation into the subretinal space of rat and primate models of retinal degeneration differentiated into a range of retinal cell types, developed a well-organised outer and inner nuclear layer and formed synaptic connections with the host retina. Patients with advanced retinal degeneration may require transplantation of RPE, photoreceptors, and/or other retinal cells, hence the generation of hESC/hiPSC-derived laminated retina presents a significant step towards the design of human clinical trials. To be able to achieve this, safe, robust and efficient differentiation methods that comply with good-manufacturing practice need to be devised. Preliminary results from stage I/II clinical trials have shown that RPE cells generated from hESCs can successfully be transplanted [16] into the subretinal space without causing adverse events in patients with AMD or Stargardt's disease, however clinical trials on transplantation of neural retinal sheets from hESC or hiPSC have not yet been performed. This is due in part to the length of current differentiation protocols (up to 250 days) [17].

Generation of retinal tissue is useful not only for transplantation purposes but also for the study of retinal diseases *in vitro*. The normal retina consists of multiple layers of neural tissue, which are in direct contact with and supported by the RPE. Both tissues are required for visual function. Several retinal diseases affect the neural retina and the RPE, yet the way in which each of these tissue types are affected, is not well understood [18]. Therefore the development of suitable protocols which result in the generation of neural retina in conjunction with RPE may be useful for studying retinal disease [19].

It is increasingly being recognised that the extracellular matrix (ECM) is important for the correct development and function of the retina both *in vivo* and *in vitro* [20–25], and changes in the ECM are associated with age-related degenerative changes in the retina including AMD [26]. Mutations affecting several components of the retinal ECM have been identified in patients with retinal disease [27–33]. Several animal models have also demonstrated how mutations in other ECM components can affect retinal ontogenesis and are associated with age-related degenerative changes [34–38]. It was hypothesised that recreation of the retinal microenvironment during hESC and hiPSC differentiation may provide the critical micro-environmental cues that are needed for their efficient differentiation to fully laminated neural retina with RPE.

The retinal ECM and Bruch's membrane (BrM), are enriched in proteoglycans [39,40]. A number of studies have shown that the major component of the retina is hyaluronic acid (HA), a large non-sulphated polysaccharide which binds a number of secreted proteins including other ECMs, such as link proteins and proteoglycans [24,40–42]. Recent work has suggested that HA-based hydrogels can drive neural [43] and retinal differentiation under 3D conditions and can also be used to deliver cells into the retina [44–48] as well as other areas of the CNS [49,50]. Similarly, RGD-alginate hydrogels appear to be promising scaffolds and have been successfully used to transplant primary foetal retinal tissue in rats [51] and to promote neural differentiation of mouse ESCs [52]. Alginate has been shown to maintain good viability of encapsulated primary and adult human RPE cell lines [53,54]. Furthermore, encapsulation in 1% alginate hydrogels has been shown to enhance the pigmented RPE phenotype of both human and porcine primary adult RPE and the expression of typical RPE markers such as RPE65 and tyrosinase [53,55]. Additionally, both alginate and HA are used in ophthalmic products, including those used intraocularly [56,57], and are well tolerated in the eye.

The addition of insulin-like growth factor 1 (IGF-1) to serum-free media has previously been shown to enhance formation of hESC-derived 3D laminated neural retina containing functional photoreceptors with membrane capabilities amenable to phototransduction [13]. Here it was investigated whether the 3D culture of hESC- and hiPSC-derived tissue, in the same defined media with IGF-1, within HA, HA/gelatin, 0.5% RGD-alginate or 1% RGD-alginate could enhance retinal differentiation compared with suspension culture in media alone. The resulting effects of hydrogel encapsulation on both RPE and neural retina formation were assessed.

2. Methods and Materials

Unless otherwise specified, all reagents were purchased from Sigma Aldrich (Dorset, UK).

2.1. Cell culture and generation of embryoid bodies (EBs)

The experimental procedure is summarised in Fig. 1. The H9 hESC line (Wicell Inc.) and SB-AD3 hiPSC line (derived and fully characterised) were cultured on growth factor reduced Matrigel-coated 6-well plates in mTeSR1 media (Stem Cell Technologies, Cambridge, UK) supplemented with penicillin-streptomycin (P/S, 1% v/v). EBs were generated by dissociating cells at 90% confluence with Accutase (Thermo Fisher Scientific) and seeding 9000 cells into each well of a 96-well lipidure-coated U-bottom plate (Amsbio, MA, USA) in 100 µl of mTeSR1 with 10 µM ROCK inhibitor (Y27632, Tocris, Bristol, UK). On day 3, media was changed to differentiation media (DMEM/F12 with 1% P/S, Thermo Fisher Scientific 20% KOSR (Thermo Fisher Scientific, Glasgow, UK), IGF-1 (5 ng/ml, R and D systems, Minneapolis, USA) and B27, Thermo Fisher Scientific). Media was changed every 3 days thereafter, with serum reduced to 15% at day 5, then 10% at day 9, before finally culturing the cells in serum-free media from day 37 onwards, supplemented with 1% P/S, 10 ng/ml IGF-1,B27 and N2 (Thermo Fisher Scientific, Glasgow, UK). EBs were maintained in 96-well plates until day 12 when they were transferred to ultra-low-attachment plates (Corning) and either kept suspension in media (controls) or encapsulated in hydrogel (0.5% RGD-alginate, 1% RGD-alginate, HA or HA/gelatin – as specified below) and cultured until day 45. Control EBs were then cultured in 3D suspension in media only throughout the duration of the experiment (45 days) as previously described [13]. Scans, photos and samples of EBs were taken at day 30 and 45 for analysis via immunohistochemistry (IHC), qRT-PCR and flow cytometry.

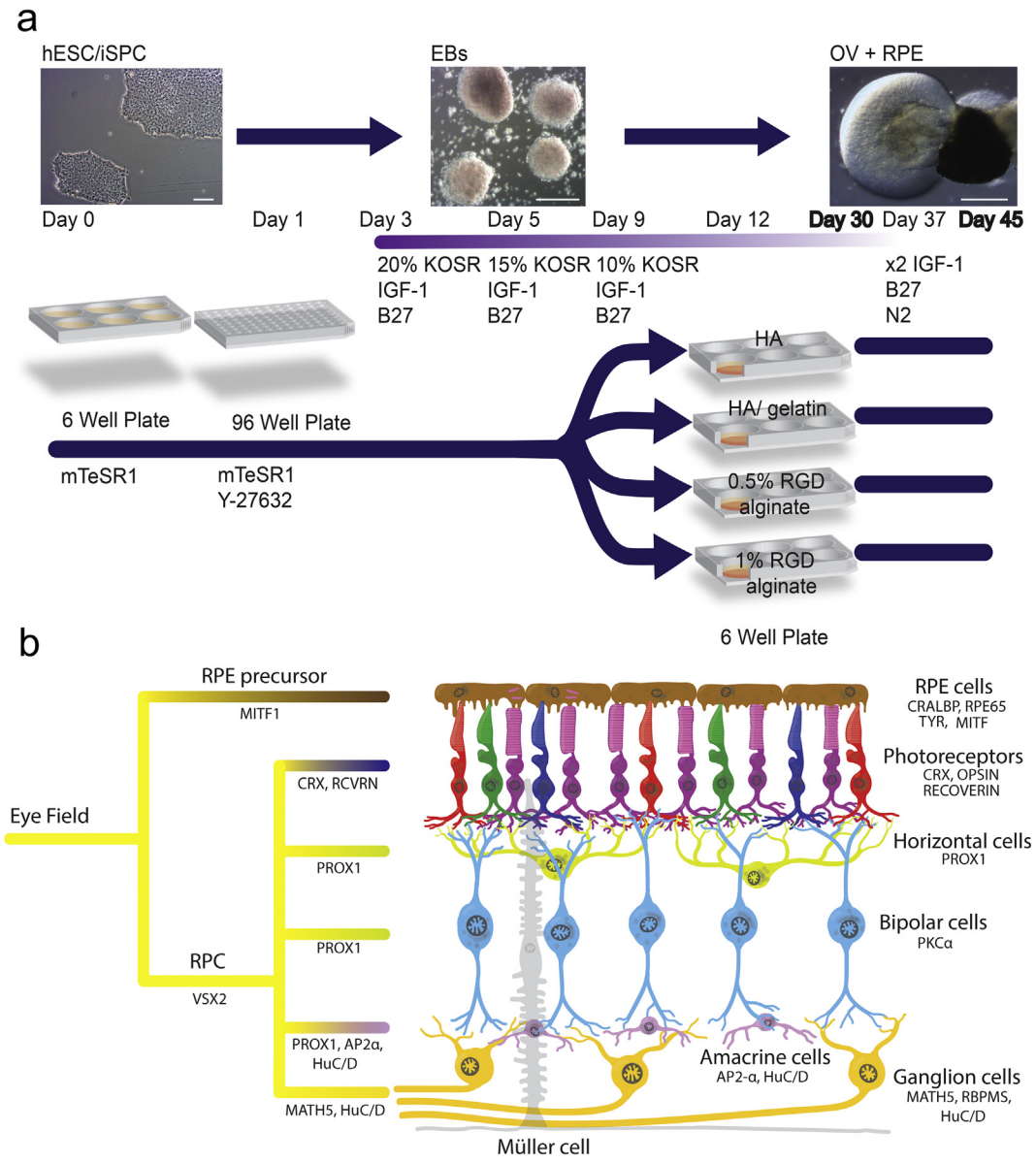

Fig. 1. a) Schematic showing the different protocols followed. hESC/hiPSC were cultured on Matrigel in mTeSR1 media, then embryoid bodies (EBs) were generated using ultra low adhesion U-shaped 96-well plates. EBs were maintained in 96-well plates until day 12 when they were transferred to petri-dishes or low attachment 6 well plates and either kept in suspension in media (controls) or encapsulated in hydrogel (0.5%/ 1% RGD-alginate, HA HA/ gelatin hydrogels) and cultured until day 45. Over time the development of phase bright tissue at the edge of EBs reminiscent of the evaginating optic vesicle (OV) were observed along with pigmented RPE foci as indicated in the 'OV + RPE' image. Scans, photos and samples of EBs were taken at 30 and 45 days. Samples were analysed via IHC, qRT-PCR and flow cytometry (full details can be seen in the Methods section), scale bar 100 μm for the left hand side panel and 500 μm for the middle and right hand panel. b) Schematic showing the progression of normal human retinal differentiation and lamination together with characteristic markers of different retinal cell types. Laminated adult human neural retina and retinal pigmented epithelium (RPE) arise from common eye field progenitor cells. These cells either go on to express MITF1 and further differentiate into RPE cells, or *VSX2*-positive retinal progenitor cells (RPCs) before differentiating into neural retinal cell types which include photoreceptors, bipolar cells, amacrine cells, Müller cells, horizontal cells and retinal ganglion cells. The expression of key phenotypic markers is indicated. These markers were used to identify retinal cells in cultures at day 30 and day 45 of differentiation.

2.2. Hydrogel preparation and EB encapsulation

Gly-Arg-Gly-Asp-Ser-Pro- (GRGDSP-) coupled high guluronic acid, high molecular weight alginate (NOVATACH MVG GRGDSP, Novamatrix, PA, USA) (RGD-alginate) was prepared to either 0.5% or 1% w/v concentration by the addition of differentiation media containing 10% w/v KOSR. 12-day old EBs were mixed with the RGD-alginate solutions, which were crosslinked by immersion in 0.1 M calcium chloride for two hours, as previously described [58]. Hystem™ (thiolated-HA) (referred to as 'HA' form hereon in) and Hystem-C™ (1:1 thiolated HA: thiolated-gelatin) (referred to as 'HA/gelatin' from hereon in) were prepared according to the manufacturer's instructions, which involved addition of the thiol reactive, Extralink™, crosslinking agent followed by incubation at 37 °C for approximately 30 min, until fully polymerised. Acellular hydrogels for rheological and Scanning Electron Microscopy (SEM) analysis were made the same way, without the addition of EBs.

2.3. Morphological characterisation of hydrogels via scanning electron microscopy (SEM)

RGD-alginate and HA-based gels were prepared according to the method described above. Samples were immediately fixed in 2% glutaraldehyde in HEPES buffered saline for one hour, then

washed in saline, rapidly frozen in liquid nitrogen and then freeze dried (Labconco, Freezone 1) with an ice condenser temperature of −55 °C for 24 h, until all the solvent sublimed. Each sample was then mounted on a carbon disk supported by an aluminium stub and coated with a 15 nm layer of gold (Polaron SEM, Coating Unit). Representative images of the hydrogel morphology were collected by SEM (Cambridge Stereoscan 240). Maximum pore diameters in SEM images of hydrogels were determined using Image J (National Institute of Health (NIH), Maryland, USA). Images were converted to 8-bit, pores were traced using the wand tool, filled, then after thresholding to show only the filled pores, the size of these regions was analysed using the analyse particles function. For all hydrogels, ⩾120 pores were analysed. It should be noted that the metrics presented are for dry scaffolds and while they are correlated to the hydrated scaffold they are not descriptive of its properties.

2.4. Mechanical characterisation of hydrogels via rheology

Rheological characterisation of hydrogels was performed using Malvern Kinexus Pro+ rotational rheometer (Worcestershire, UK) which is equipped with a temperature control stage. Samples of 20 mm in diameter with planar surfaces were cast in stainless steel moulds, as described above. 20 mm diameter serrated parallel plates were used to avoid slippage. The thickness of samples was 2.3–2.5 mm. The plate gap was set to be identical to the sample thickness. A special solvent trap system was used to avoid dehydration of the sample. To identify the linear viscoelastic region (LVR), oscillatory strain sweep tests were applied between 0.01% and 10%. Frequency sweep tests were then performed between 0.1 Hz and 10 Hz at 0.1% which was within the LVR. The storage (elastic component) modulus (G′), loss (viscous component) modulus (G″) and dynamic viscosity (η^*) were extracted to assess the mechanical spectra of the gels at 37 °C. Detailed comparisons of G′, G″ and η^* were made between gels at a frequency of 1 Hz.

2.5. Quantitative assessment of retinal determination in 3D culture

For each experimental condition, the total number of EBs with phase bright OVs as described in a recent publication [13], and/or any pigmented RPE foci were counted under a dissection microscope on days 30 and 45 of differentiation. 134 ± 7 EBs were counted for each sample. This analysis was repeated by a second experienced person to ensure an objective evaluation across all culture conditions.

2.6. RNA extraction, RT and qRT-PCR

20–50 EBs were homogenised using a pestle and mortar and RNA was extracted using a tissue extraction kit (*Promega, USA*) as per the manufactures instructions. 1 μg of RNA was reverse transcribed using random primers (*Promega, USA*). qRT-PCR was performed using a Quant Studio 7 Flex system (Applied Biosystems, USA) with SYBR Green (*Promega, USA*). Each primer (listed in Table 1) was used at a concentration of 1 μM, and at a ratio of 50:50 for forward and reverse. The reaction parameters were as follows: 95 °C for 15 min to denature the cDNA and primers, 40 cycles of 94 °C for 15 s followed by primer specific annealing temperature for 30 s, succeeded by a melt curve. A comparative C_t method was used to calculate the levels of relative expression, whereby the C_t was normalised to the endogenous control (*GAPDH*). This calculation gives the ΔC_t value, which was then normalised to a reference sample (i.e. a positive control), giving the $\Delta\Delta C_t$. The fold change was calculated using the following formula: $2\text{-}\Delta\Delta C_t$.

2.7. Flow cytometry

EBs were dissociated in a 1:1 mix of Accumax™ (Merk Millipore, Hertfordshire, UK) and TrypLE™ (Thermo Fisher Scientific, Glasgow, UK) at 37 °C for 60 min, with agitation every 10 minutes. Cells were collected and fixed in 4% paraformaldehyde (PFA) in PBS at 37 °C for 10 minutes then washed in PBS and stored in 90% methanol in PBS at -20 °C before analysis. Cells were blocked in PBS containing 2% bovine serum albumin (BSA) and 2% normal goat serum for one hour at room temperature. Primary antibodies were diluted as stated in Table 2 and incubated with the cells for one hour in PBS with 0.5% BSA. After two washes in PBS, cells were incubated in secondary antibodies (Alexafluor™ goat-anti-rabbit 647 and goat-anti-mouse 488), (Thermo Fisher Scientific, Glasgow, UK), diluted 1/800 in PBS with 0.5% BSA, at room temperature for one hour, before washing and suspending the cells in PBS with 10% v/v DAPI. Cells were then analysed via flow cytometry (BD FACSCanto™, BD Biosciences, CA, USA).

2.8. Immunohistochemistry (IHC)

EBs were collected on days 30 and 45 of differentiation and IHC analysis performed on cryostat sections as described previously [13]. A panel of antibodies listed in Table 2 were used for this analysis. At least ten EBs were sampled from each differentiation condition on days 30 and 45 for analysis. Images were obtained using a Zeiss Axio Imager.Z1 microscope with ApoTome.2 accessory equipment and AxioVision software (Zeiss, Oberkochen, Germany).

2.9. Quantification of pigmented RPE foci

The area occupied by pigmented RPE foci were non-destructively determined similarly to the method previously described [58]. Dishes containing 3D EB structures were scanned at day 30 and 45 (Epson Perfection V200) at 600 DPI resolution. The resulting 2D scans were analysed in ImageJ (NIH, Maryland, USA). EBs were manually outlined at high magnification so that the total area occupied by EBs could be determined. Scans were converted to saturation density using the Colour Transformer plugin. A threshold was then applied so that only pigmented RPE foci were shown (as indicated in Fig. 6a). The area occupied by pigmented RPE foci was measured so that the percentage of the total number of EBs within the culture which were pigmented could be determined i.e.% pigmentation = (area of pigmented RPE foci/total area occupied by EBs) × 100. Although RPE and EBs were 3D structures and not a monolayer, the quantification of % area occupied by RPE within the EBs from 2D images was assumed to reflect the differences in volume occupied by the RPE between samples.

2.10. Statistical analysis and data presentation

All analysis was performed using the open access statistical software R Project (R Foundation for Statistical Computing, Vienna, Austria), and significance was set at a p-value < 0.05. In all experiments, statistical significance was determined using generalised linear models (GLMs). Using GLMs allowed quantification of the effect size of the various input variables (time in culture, cell type, hydrogel type) on the response variable (e.g., specific gene expression) as, for example, is similarly described in a recent paper [59]. The model used was lm (response variable ~ cell type + hydrogel condition + time point). A power analysis determined the sample number sufficient to identify significant differences with 95% confidence and 80% power. All samples were performed in replicates of three or more, and data presented as mean ± SEM, unless otherwise stated. Since at least three biological replicates were performed for each cell type, under each experimental condition and

Table 1
DNA oligonucleotides used for qRT-PCR.

Gene	Forward primer	Reverse primer
GAPDH	TGCACCACCAACTGCTTAGC	GGCATGGACTGTGGTCATGAG
VSX2 (CHX10)	GGCGACACAGGACAATCTTTA	TTCCGGCAGCTCCGTTTTC
MITF1	TTCACGAGCGTCCTGTATGCAGAT	TTGCAAAGCAGGATCCATCAAGCC
RCVRN	TTCAAGGAGTACGTCATCGCC	GATGGTCCCGTTACCGTCC
CRX	GTGAGGAGGTGGCTCTGAAG	CTGCTGTTTCTGCTGCTGTC
RPE65	GCCCAGGAGCAGGACAAAAG	GCGCATCTGCAAGTTAAAACCA
TYR	TAGCGGATGCCTCTCAAAGC	CAATGGGTGCATTGGCTTCT
MATH5	CCCTAAATTTGGGCAAGTGAAGA	CAAAGCAACTCACGTGCAATC
PROX1	TGACTTTGAGGTTCCAGAGAGA	CTCTTGTAGGCAGTTCGGGG
AP2α	GTTACCCTGCTCACATCACTAG	TCTTGTCACTTGCTCATTGGG

Table 2
Antibodies used for immunolabelling cells for flow cytometry and immunohistological analysis showing dilutions used.

Protein	Supplier	Cat. number	Dilution (Flow cytometry)	Dilution (IHC)
CRALBP	Source Bioscience	GTX15051	1/100	1/200
VSX2 (CHX10)	Sigma Atlas	HPA003436	1/100	1/50
Cleaved caspase 3	New England Biolabs	9661S	1/100	1/200
Ki-67	Abcam	ab15580	1/100	1/200
RBPMS	PhosphoSolutions	1830-RBPMS	1/400	1/200
RCVRN	Millipore	AB5585	1/100	1/800
HuC/D	Invitrogen (Molecular probes)	A21271	1/800	1/200
AP2α	Santa Cruz Biotechnology	sc-184	1/100	1/100
COL-IV	Abcam	ab6586	1/100	1/250

sampled at two differentiation time points, a total of 60 samples were used in each statistical model. Graphs were prepared in Prism (GraphPad, CA, USA) from the raw data.

3. Results

The effect of hydrogel encapsulation on retinal differentiation of hESC- and hiPSC-derived EBs under serum-free defined conditions was assessed using a combination of techniques including qRT-PCR, IHC and flow cytometry. Four different hydrogels were used to encapsulate EBs generated from hESCs and hiPSCs; 0.5% RGD-alginate, 1% RGD-alginate, HA and HA/gelatin (Fig. 1a). The specific details of these hydrogels are given in the methods section. In preliminary work, normal alginate lacking the RGD motif was also investigated, but unfortunately culture in this alginate resulted in a reduction in the percentage of retinal structures and in the appearance of numerous abnormal cystic structures (data not shown). Furthermore, in normal alginate, many EBs dissociated, indicative of reduced cell viability. We therefore used RGD-alginate in this study, which is widely used in tissue engineering, and has previously been shown to enhance the viability of mesenchymal stem cells.

EBs were encapsulated on day 12 upon transfer from 96-well dishes into low attachment 6-well plates and the differentiation of EBs towards a retinal phenotype was assessed at day 30 and 45 (Fig. 1a). The ability of EBs to form 3D laminated neural retina with retinal pigmented epithelium (RPE) was assessed and compared between the different hydrogels and controls (suspension culture in media only with no hydrogel). A schematic showing how native laminated retinal tissue arises from common progenitor cells, with key markers used to identify emergence of the different cell types, is shown in Fig. 1b.

3.1. Hydrogel characterisation

A comparison of mechanical and microstructural properties of hydrogels was made using SEM imaging and rheology and described in the supplementary section (Suppl. Figs. 1 and 2 and accompanying text).

3.2. Hydrogel encapsulation maintained high cell viability and the ability of EBs to generate retinal tissue

Over time the development of phase bright tissue at the edge of EBs reminiscent of the OVs was observed (Fig. 2a), along with pigmented RPE foci which, under high power magnification, showed the typical hexagonal RPE morphology. EBs displaying OVs which lacked RPE, EBs containing both OVs and pigmented RPE foci, or EBs lacking OVs but displaying RPE foci alone were observed and quantified under all five conditions. Examples of EBs displaying the simultaneous occurrence of OVs with pigmented RPE are shown for both hESC- and hiPSC- derived cultures under each condition in Fig. 2a. EBs appeared to remain healthy and viable under all five conditions throughout the course of the experiment upon visual examination. The number of cells in which expressed the apoptotic marker cleaved-caspase-3 (CASP-3) was measured by flow cytometry to assess the level of cell death under each condition for both hESC and hiPSC-derived EBs at day 45, when the experiment was terminated (Fig. 2b). Levels of apoptosis were low in all samples and the number of CASP-3-positive cells was not significantly different between hydrogel and control samples, showing that hydrogel encapsulation had no adverse effect on cell viability ($p > 0.05$). The low numbers of CASP-3 expressing cells under all conditions was also confirmed by IHC, and a representative image is shown in Fig. 2c. Furthermore, EBs were seen to increase in size throughout the course of the experiment in all hydrogels as they did in controls, and proliferating cells (expressing Ki-67) were frequently observed within developing retinal tissue at both day 30 and day 45. A representative image showing the IHC staining obtained for Ki-67 is shown in Fig. 2d.

3.3. Occurrence of OVs and pigmented RPE foci is increased by RGD-alginate hydrogels

To determine whether hydrogel encapsulation affected the propensity of EBs generated from hESCs and hiPSCs to generate retinal tissue, was compared between hydrogel conditions and controls (Fig. 3). As described in the methods, statistical analysis was performed using a linear model, and therefore all data is

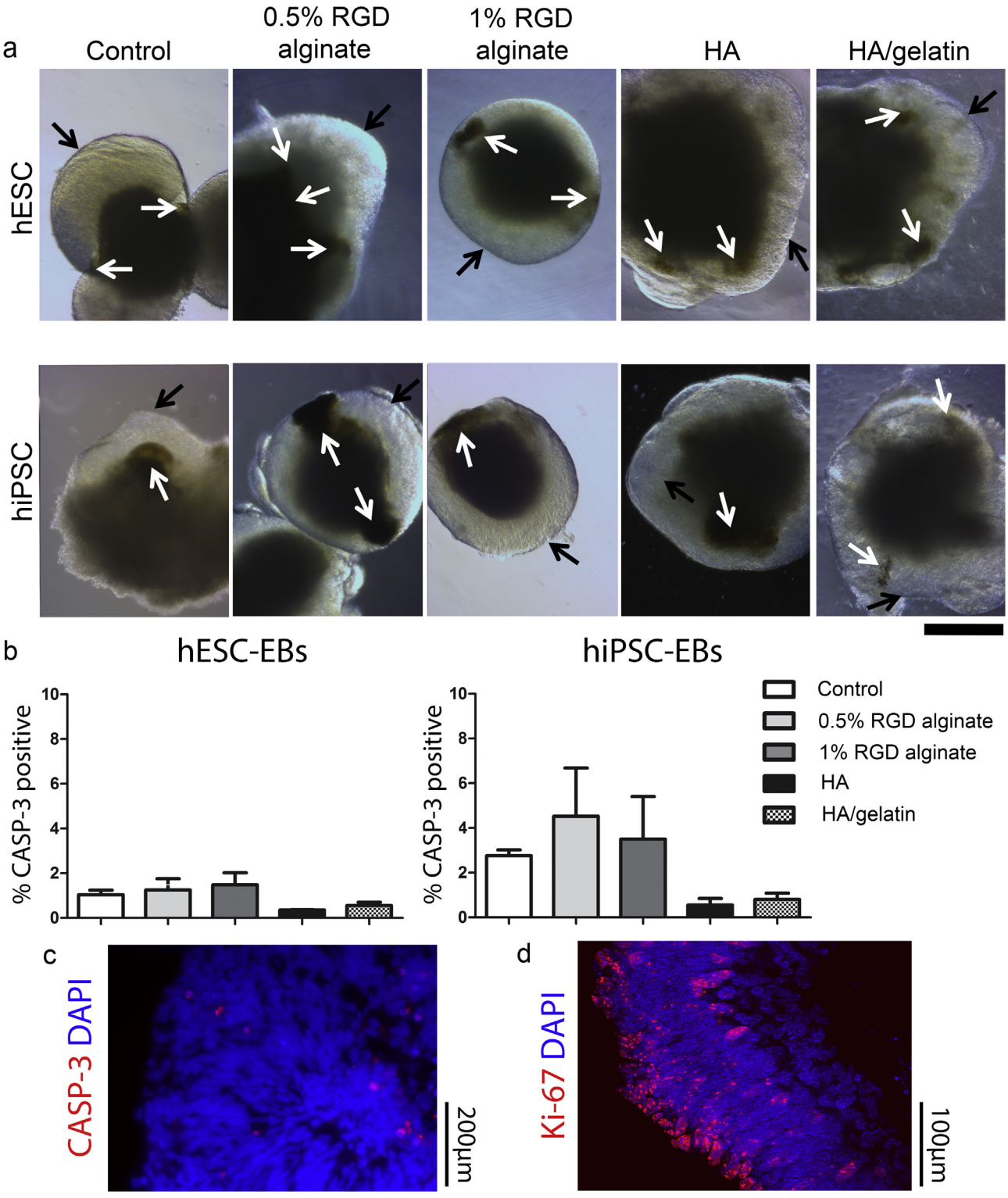

Fig. 2. Encapsulation of EBs in hydrogels does not affect cell viability or adversely impact the emergence of phase bright OVs and RPE. a) Representative examples of EBs which had developed both OV and pigmented RPE foci from hESCs and hiPSCs at day 45 under control conditions and in 0.5% RGD-alginate, 1% RGD-alginate, HA, HA/ gelatin hydrogels. Pigmented RPE foci are indicated by white arrows, while OVs under all five conditions are indicated with black arrows (Scale bar = 200 μm). b) Percentage of cells derived from hESCs and hiPSCs in all five conditions which expressed cleaved caspase-3 (CASP-3) as measured by flow cytometry at day 45, indicating that levels of apoptosis were low under all conditions and comparable between conditions ($p > 0.05$). c) Levels of CASP-3 (apoptosis marker) expression in hiPSC- and hESC-derived EBs were observed by IHC at both day 30 and day 45 and representative image is shown, confirming the low expression seen by flow cytometry in panel b. d) Viability of cells was further indicated by high numbers of proliferating (Ki-67-positive) cells within EB-derived OVs at days 30 and 45 for all samples. A representative image is shown.

considered together so that consistent effects, which are likely to be real and repeatable, are identified. In each case the effect of time in culture, the hydrogel condition (compared with control) and the cell type on the occurrence of retinal structures was determined, similarly to the qRT-PCR and other quantifications that follow.

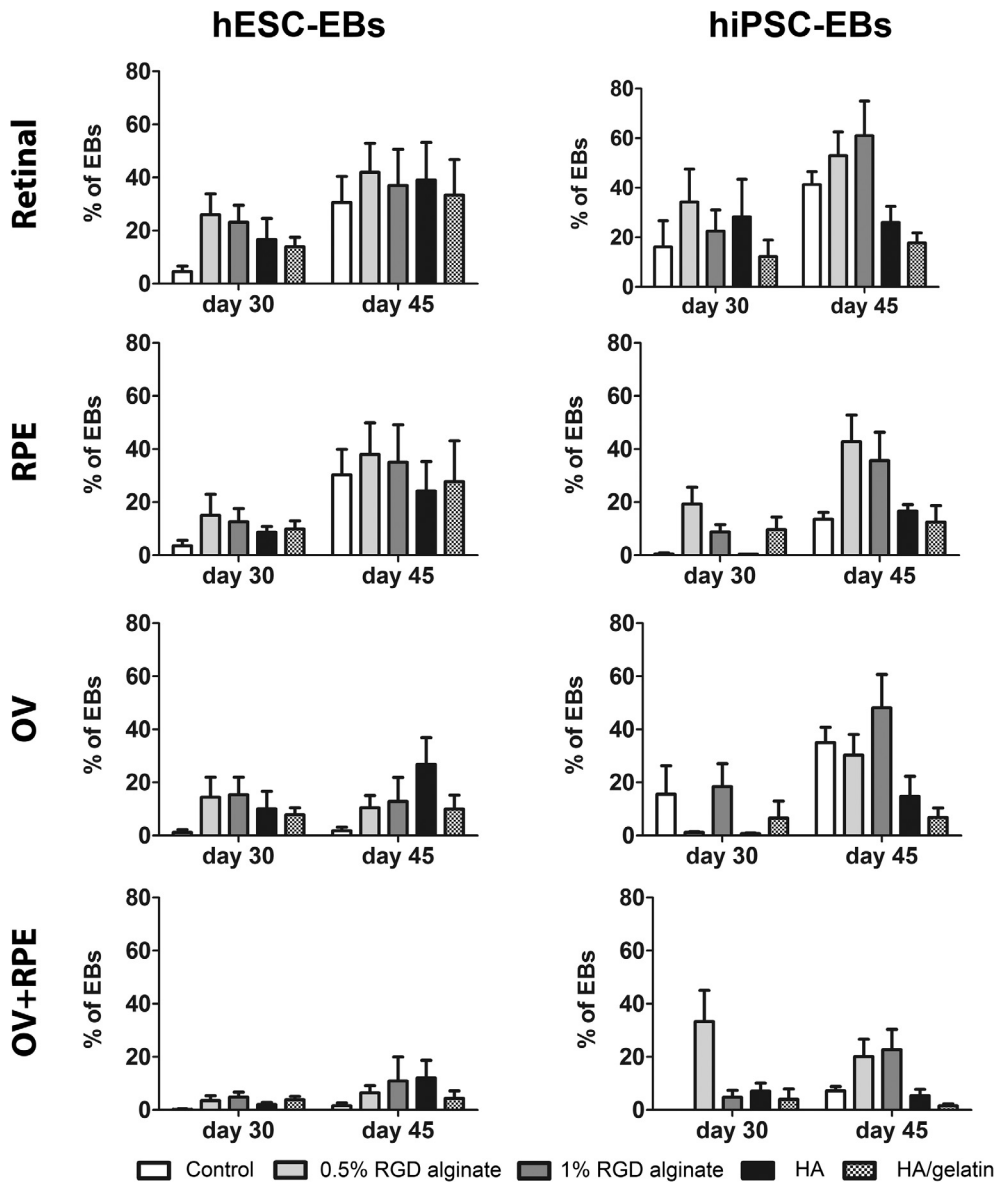

Fig. 3. Effects of hydrogel encapsulation on the hESC/hiPSC retinal differentiation. Quantitative assessment of retinal structures at day 30 and 45 derived from hESCs or hiPSCs cultured in 0.5% and 1% RGD-alginate, 1%, HA, HA/ gelatin hydrogels compared with 3D suspension culture in media only (control). All values are stated as the % of the total population of EBs. The percentage of EBs with OVs and/or pigmented RPE foci (total retinal); the % of EBs with pigmented RPE foci (with or without OV); the % EBs with OVs (with or without RPE); and % EBs with both pigmented RPE foci and OV together are shown. The percentage of EBs with emerging OVs and RPE foci together, as well as EBs with RPE foci (with or without OVs) were significantly increased by both 0.5% and 1% RGD-alginates ($p < 0.05$). 1% RGD-alginate also significantly increased the % of EBs with OVs ($p < 0.05$). All measures were significantly increased at day 45 compared with day 30 ($p < 0.05$) and the percentage of EBs with OVs was increased in hiPSCs compared with hESCs. No other significant differences were found. This implied that both alginate hydrogels increased retinal differentiation compared with control conditions.

The total number of EBs with either RPE and/or OVs (total retinal) (Fig. 3) was found to be significantly increased by both 0.5% and 1% RGD-alginate hydrogels (17% and 15.5% respectively; $p < 0.05$) compared to controls ($p < 0.05$), but was not significantly affected by the HA and HA/gelatin hydrogels ($p > 0.05$). This increase in the total retinal group is evident in both hESC and hiPSC cultures at both day 30 and day 45, although the magnitude varied between sub-groups. Furthermore, the percentage of EBs displaying either RPE and/or OVs was increased at day 45 by an average of 21% compared with day 30 ($p < 0.05$). Although the appearance of retinal structures appeared slightly increased in hiPSCs compared with hESCs, this increase was not significant ($p > 0.05$).

Similarly, the total number of EBs containing pigmented RPE foci (either with or without OVs) (Fig. 3) was also significantly increased in 0.5% RGD-alginate by an average of 17% ($p < 0.05$) and in 1% RGD-alginate by an average of 13.5% ($p < 0.05$), and unaffected by HA-based hydrogels ($p > 0.05$). Again, this increase is evident at both time points for both cell types to different degrees. The percentage of EBs displaying RPE, was increased by an average of 20% at day 45 compared with day 30, but not significantly different between hESCs or hiPSCs ($p > 0.05$).

The percentage of EBs with OVs (either with or without simultaneous RPE) (Fig. 3) was significantly increased in 1% RGD-alginate by an average of 14%, ($p < 0.05$). No significant increases in total OV numbers were seen in the other hydrogels, including 0.5% RGD-alginate ($p > 0.05$). Numbers of OVs were increased by an average of 8.5% at day 45 compared with day 30 ($p < 0.05$) and hiPSCs generated on average 10% more OVs than hESCs ($p < 0.05$).

The simultaneous appearance of OVs along with pigmented RPE in the same EB (Fig. 3) was increased by 0.5% RGD-alginate and 1%

RGD-alginate by an average of 7.5% and 12%, respectively ($p < 0.05$) but not significantly affected by the HA or HA/gelatin hydrogels ($p > 0.05$). At day 45 the number of EBs with OVs and RPE together was increased by 7.5% on average, compared with day 30 ($p < 0.05$). No significant differences in total numbers of OVs were seen between the hiPSCs or hESCs ($p > 0.05$). Overall, the quantitative assessment performed over day 30 and 45 of differentiation suggest that both 0.5% and 1% RGD-alginate can enhance retinal differentiation of hESCs and hiPSCs.

3.4. 5% RGD-alginate hydrogels enhanced RPE formation in 3D retinae derived from hESCs and hiPSCs

The results shown in Fig. 3 indicate that both 0.5% and 1% RGD-alginate could increase the formation of RPE from hESCs and hiPSCs. To validate this finding, qRT-PCR analysis was performed on hESC- and hiPSC-derived retinal tissue on days 30 and 45 of differentiation (Fig. 5) with RPE markers characterising the early (*MITF1*) and definitive commitment of retinal progenitor cells to an RPE phenotype (*TYR* and *RPE65*). Interestingly, *MITF1* expression dropped dramatically between day 30 and 45 for hiPSC-derived cultures, but was relatively low at both day 30 and day 45 in hESC cultures (Fig. 5). Overall, the expression of *MITF1* was not significantly different from controls in any of the hydrogels ($p > 0.05$). *RPE65*, a definitive marker of RPE, was found to be significantly increased in 0.5% RGD-alginate ($p < 0.05$), when compared with controls (Fig. 4). Expression of *RPE65* was not significantly affected by 1% RGD-alginate, HA or HA/gelatin hydrogels ($p > 0.05$). *RPE65* expression was significantly increased at day 45 compared with day 30 ($p < 0.05$), where expression was seen to be up to 4-fold higher than normal human RPE. *RPE65* expression was also significantly higher in hiPSC- compared with hESC-derived cultures ($p < 0.05$).

Expression of *TYR*, another marker of RPE cells and which codes for one of the proteins essential for pigment synthesis was also analysed via qRT-PCR (Fig. 4). Expression of *TYR*, similarly to *RPE65* was significantly increased in 0.5% RGD-alginate samples compared with controls ($p < 0.05$), with no significant differences for any of the other hydrogels, including 1% RGD-alginate ($p < 0.05$). Together these qRT-PCR results supported the finding that 0.5% RGD-alginate enhances RPE formation compared with controls, as suggested by the quantitative analysis in Fig. 3, and that HA and HA/gelatin have no significant effect on RPE formation. However, the qRT-PCR results did not support the finding that 1% RGD-alginate increased RPE formation reported in the previous Results section.

To further investigate whether RGD-alginate hydrogels could enhance RPE formation, analysis of the area occupied by pigment in scanned images of hESC and hiPSC-derived EBs at day 30 and 45 was assessed (Fig. 5a and b). From the image analysis it was found that, in agreement with all other data, the formation of pigmented RPE was not increased by either HA or HA/gelatin hydrogels ($p > 0.05$) and that 0.5% RGD-alginate, but not 1% RGD-alginate hydrogel, significantly increased pigmented RPE formation ($p < 0.05$). Visually this is clearly evident for hESCs and hiPSCs at both day 30 and 45. Furthermore, flow cytometric analysis (Fig. 5c) showed that at day 45 0.5% RGD-alginate alone significantly increased the percentage of RPE cells as revealed by staining with *anti*-CRALBP, a marker of definitive RPE ($p < 0.05$).

3.5. Neural retinal formation was similar across all conditions

Quantitative assessment of retinal structures (Fig. 3) implied that, in addition to RPE, the formation of neural retina was also enhanced by encapsulation in the 1% RGD-alginate hydrogel. In an attempt to validate this finding the expression of various neural retinal markers were measured by qRT-PCR (Fig. 6).

The qRT-PCR analysis showed that the expression of *VSX2 (CHX10)*, a marker of neural retinal progenitor cells, was unaffected by hydrogels compared with controls ($p < 0.05$). This indicated that the number of progenitors was not significantly affected by culture of cells in any hydrogel, compared with control conditions (Fig. 6). The overall expression of *VSX2* was, however, significantly increased in hiPSC-derived tissue compared with that of hESCs ($p < 0.05$) with the fold change being around 10 times higher at both day 30 and day 45. This correlated with the increased number of *VSX2* positive cells in hiPSC derived retinae when compared to hESC as detected by flow cytometric analysis at day 45 (Fig. 7a, $p < 0.05$). Flow cytometric analysis of *VSX2* expression also confirmed that the number of retinal progenitor cells was not significantly affected by any of the hydrogels at day 45 compared with controls (Fig 7a, $p > 0.05$).

Retinal ganglion cells are the first cells to mature in the normal retina, and to measure emergence of retinal ganglion cells in culture, the expression of *MATH5* was assessed by qRT-PCR in both hESC- and hiPSC-derived EBs (Fig 6). *MATH5* was found to be significantly increased in 0.5% RGD-alginate cultures compared with controls ($p < 0.05$), while other hydrogels had no significant effect ($p > 0.05$). The increased numbers of retinal ganglion cells was also confirmed by flow cytometric analysis of RBPMS (a selective marker of retinal ganglion cells in the mammalian retina)-positive cells in the hiPSC-derived EBs (Suppl. Fig. 3).

Following the emergence of retinal ganglion cells, the emergence of other retinal neurons was expected, in accordance with the order of human retinal histogenesis (Fig. 1b). To assess whether the emergence of other retinal phenotypes was affected by culture in the hydrogels compared with controls, qRT-PCR was used to compare the expression of *PROX1* (horizontal cells), *AP2α* (amacrine cells) and *CRX* and *RCVRN* (photoreceptor progenitors) (Fig. 6). The expression of all of these genes was unaffected by any of the hydrogels compared with controls ($p > 0.05$), indicating that enhanced RPE formation in neural retina, as indicated in Fig. 4 and 5, was not at the expense of neural retinal development. Interestingly, the expression of *CRX* and *RCVRN* ($p < 0.05$) was significantly increased in hiPSC- versus hESC-derived tissue, corroborating the findings above indicating increased *VSX2* expression (Fig. 1a).

IHC was performed on sections of EBs from both hESCs and hiPSCs sampled on days 30 and 45 under all conditions (hydrogels and controls) to confirm the presence multiple retinal phenotypes as indicated by qRT-PCR and flow cytometric analysis (Fig. 6, 7a and Supp. Fig. 3). Representative examples of developing laminated retina are shown in Fig. 7b. The IHC revealed that laminated retina could form under all experimental conditions, as indicated by the presence of HuC/D on the basal layer (towards the centre of the EB) which is expressed by developing retinal ganglion cells and amacrine cells of the inner neural retina, and large numbers of *VSX2*-positive neural retinal progenitor cells throughout the outer (apical) region of the OVs. Furthermore, a basement membrane-like structure which was rich in collagen-IV (COL-IV) formed along the basal surface of OVs, reminiscent of an inner limiting membrane (ILM) of native retina. The emergence of photoreceptors under all conditions was suggested by the presence of RCVRN positive cells, outlining typical elongated photoreceptor morphology. RCVRN is also a marker of cone bipolar cells, but since these cells arise much later than cone photoreceptors, we expect the cells labelled were photoreceptor precursors.

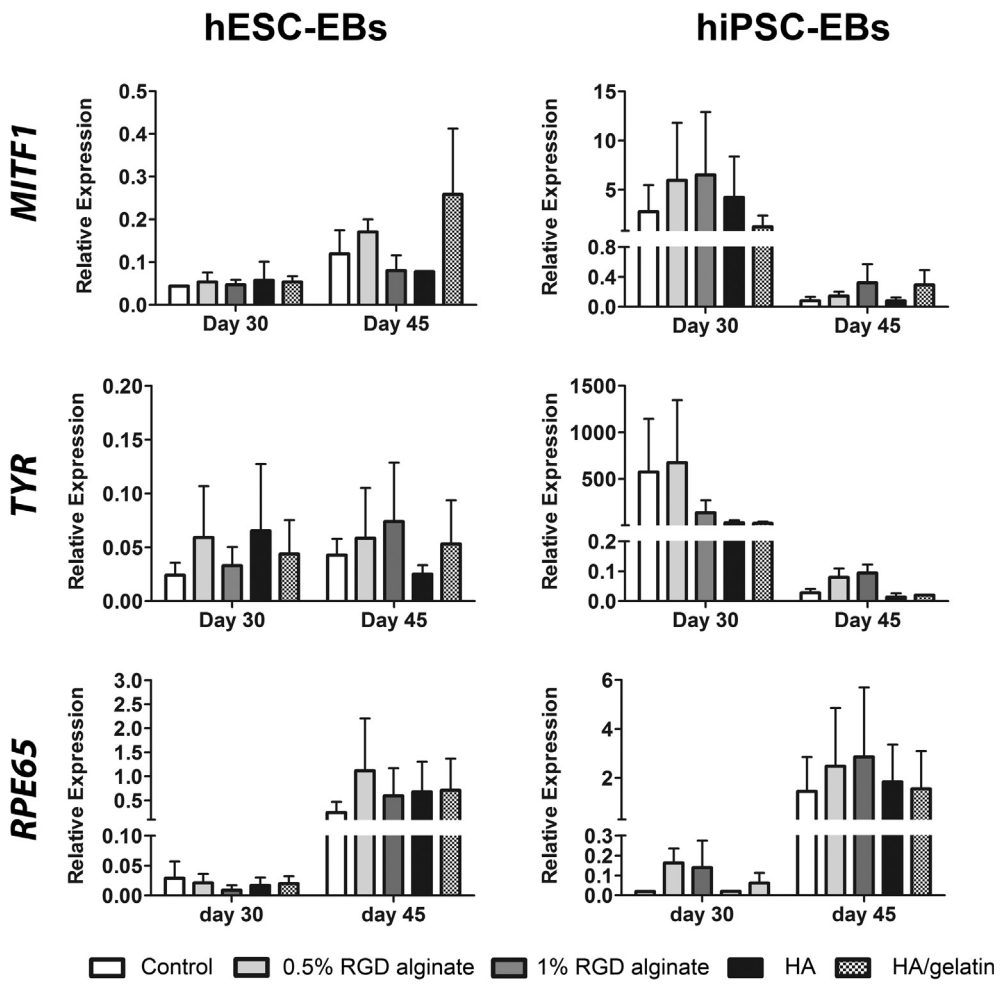

Fig. 4. Quantification of RPE-specific gene expression. Expression of *MITF1*, *TYR* and *RPE65* at days 30 and 45 in hESC- and hiPSC-derived EBs as determined by qRT-PCR. *GAPDH* was used as the housekeeping gene. All samples were normalized to adult human RPE. No significant differences were seen in *MITF1* expression levels ($p > 0.05$) across conditions, however the expression of *TYR* and *RPE65* were significantly increased in EBs differentiated within 0.5% RGD-alginate ($p < 0.05$). 1% RGD-alginate, HA and HA/gelatin had no effect on RPE gene expression ($p > 0.05$). This suggested that RPE differentiation was enhanced by 0.5% alginate.

4. Discussion

Overall the results of this study demonstrate that the 0.5% RGD-alginate scaffold enhanced the initial generation of 3D-derived retinal tissue containing RPE from hESCs and hiPSCs. This is the first study to the best of the authors' knowledge which has shown that 3D culture with a biomaterial scaffold can improve the generation of retinal tissue from hESC and hiPSC. Firstly, 0.5% RGD-alginate hydrogel enhanced the development of RPE, as shown by increased occurrence of pigmented RPE foci occupying a larger area; increased expression of RPE markers (*RPE65*, *TYR*); and increased percentage of CRALBP-positive cells. Furthermore, the emergence of OVs and RPE occurring simultaneously within the same EB was significantly increased in 0.5% RGD-alginate hydrogels. qRT-PCR analysis for multiple markers of neural retinal cells (*VSX2, AP2α, PROX1, CRX, RCVRN*), along with flow cytometric analysis of *VSX2* suggested that RPE was not being preferentially generated at the expense of neural retina, with no significant effects of the 0.5% RGD-alginate on the expression of these markers. This supported the finding that the total number of OVs generated was unaffected by 0.5% RGD-alginate hydrogel, compared with the control. Additionally, qRT-PCR analysis of *MATH5* expression levels suggested that the generation of retinal ganglion cells was enhanced in 0.5% RGD-alginate hydrogels compared with controls. Since retinal ganglion cells are the first cells to arise in the native human retina this may suggest that the maturation of the neural retina is accelerated by culturing EBs in 0.5% RGD-alginate hydrogels compared with suspension culture in media alone. Longer term cultures are necessary to confirm whether later stages of retinal development can also be enhanced using 0.5% RGD-alginate scaffolds.

The number of EBs containing phase bright OV-like regions occurring with our without RPE was also significantly increased by culture in 1% RGD-alginate, however no other significant improvements were observed. This suggested that although RGD-alginate hydrogels in general may enhance retinal differentiation, the concentration of the RGD-alginate scaffold is important for optimum results. No significant improvements in any of the measures of retinal differentiation were seen for HA or HA/gelatin scaffolds showing that the derivation of retinal tissue was not improved by these scaffolds. Interestingly, according to many measures, the hiPSCs showed increased generation of retinal derivatives compared with hESCs, including: increased numbers of *VSX2*-expressing retinal progenitor cells; increased expression of photoreceptor markers; increased number OVs; and increased expression of the mature RPE marker, *RPE65*. This is not surprising since differences between different human pluripotent cell lines have previously been reported [60] [61], along with differences in their propensity to generate both retinal [62–65] and other cells and tissues [66,67].

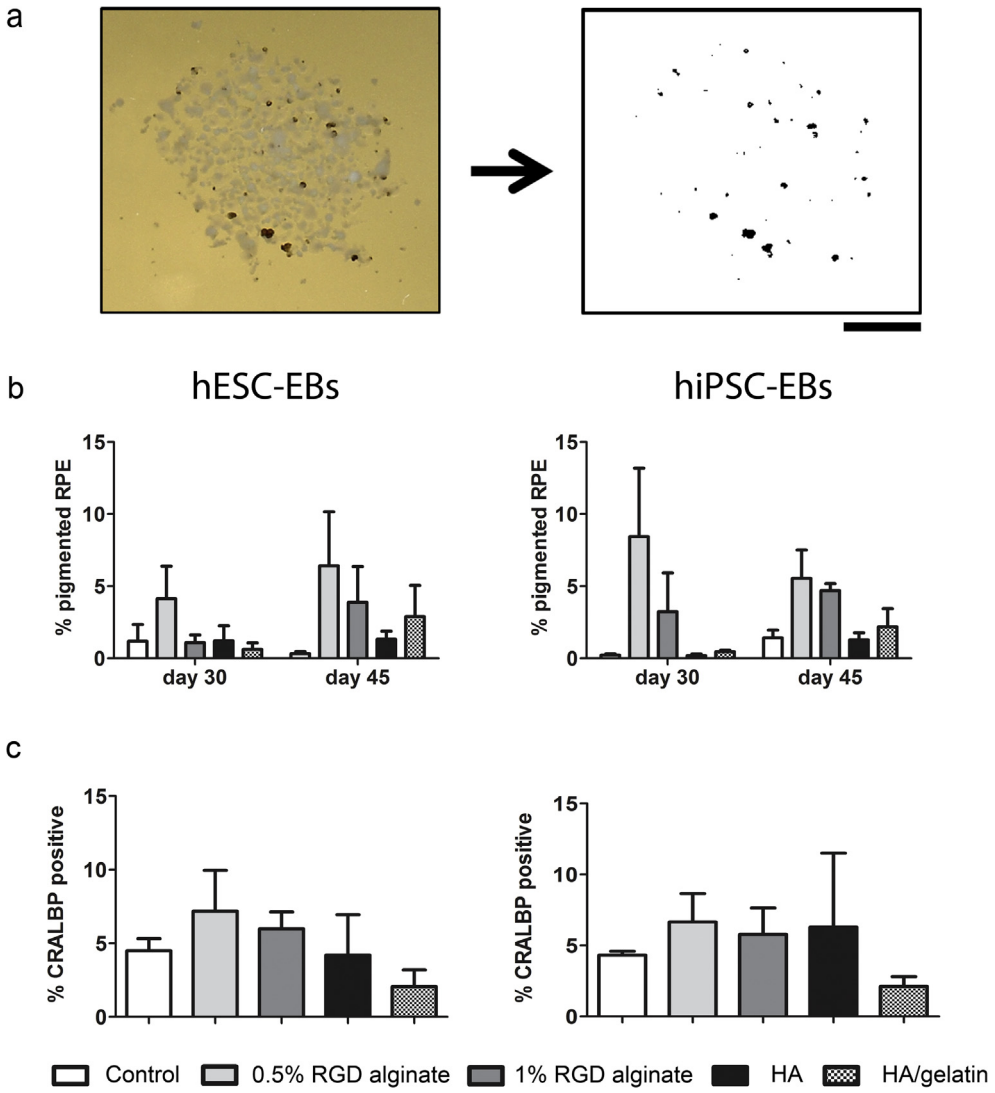

Fig. 5. The area occupied by pigmented RPE in scanned images of differentiating EBs and the number of CRALBP-positive cells were increased by encapsulation in 0.5% RGD-alginate. a) Example showing how a scanned image (left) was thresholded to allow for quantification of the observable pigmented area (right). (Scale bar = 5 cm). b) Graphs showing the% of the area taken up by EBs which was occupied by pigmented RPE in EBs derived from hESCs and hiPSCs. The % area of pigmented RPE was significantly increased by 0.5% RGD-alginate compared with control conditions ($p < 0.05$). Results across both sample day and cell type were comparable ($p > 0.05$). c) The percentage of cells expressing CRALBP as determined by flow cytometry at day 45 in hESC- (left) and hiPSC-derived (right) EBs. The number of CRALBP positive cells (expressed by RPE cells) in differentiating cultures was significantly increased by 0.5% RGD-alginate only ($p < 0.05$). This demonstrated that there was more RPE in 0.5% RGD-alginate-encapsulated EBs compared with controls, and supports the qRT-PCR analysis shown in Fig. 5.

The method of EB generation may impact on the efficiency of retinal differentiation and it is for this reason that in the present study a single method of EB generation was used, namely the 96-well plate method, which have been utilised in several other studies [22,68–70]. This allowed for the effect of hydrogel scaffolds to be assessed with homogenously sized EBs which could be grown in large quantities with ease, enabling quantitative assessment of various measures of retinal ontogenesis. Notwithstanding this, the impact of 0.5% RGD-alginate on retinal differentiation was also observed when EBs were prepared using other methods (data not shown). Comparison of the use of 0.5% RGD-alginate and serum-free media to generate retinal tissue with other published results is challenging since the efficacy of different methods is sometimes difficult to determine and this is further compounded by the complexity and variability of methods used to induce differentiation [12,71–74]. Often the expression of differentiation markers in the engineered tissue is not compared with native tissue, and is instead compared with the immortalised human RPE cell line, ARPE19, which is an imperfect alternative with several key differences compared with native RPE, including: a lack of pigment RPE; rapid proliferation; elongated cell shape; differential secretion of growth factors and differentiation markers [75–78]. It is for this reason that all qRT-PCR analysis in this study was normalized to primary human RPE or retina.

Previous work [53–55] has shown that alginate hydrogel supports the maintenance of a normal pigmented RPE phenotype, and reverses the de-differentiation that is normally seen upon *in vitro* culture. The present study has also shown that RGD-alginate hydrogels support pigmented RPE formation from pluripotent stem cells. For clinical application to restore RPE monolayer defects, RPE generated in EBs could be micro-dissected from EBs, enzymatically dissociated and seeded onto a scaffold for transplantation or injected in suspension, for example as performed in recent clinical trials [16]. Indeed, RPE cells isolated from the EBs generated in 0.5% RGD-alginate at 60 days plated onto Matrigel coated 24-well inserts of 30mm^2 area formed a deeply pigmented monolayer with typical RPE morphology (Suppl. Fig 4).

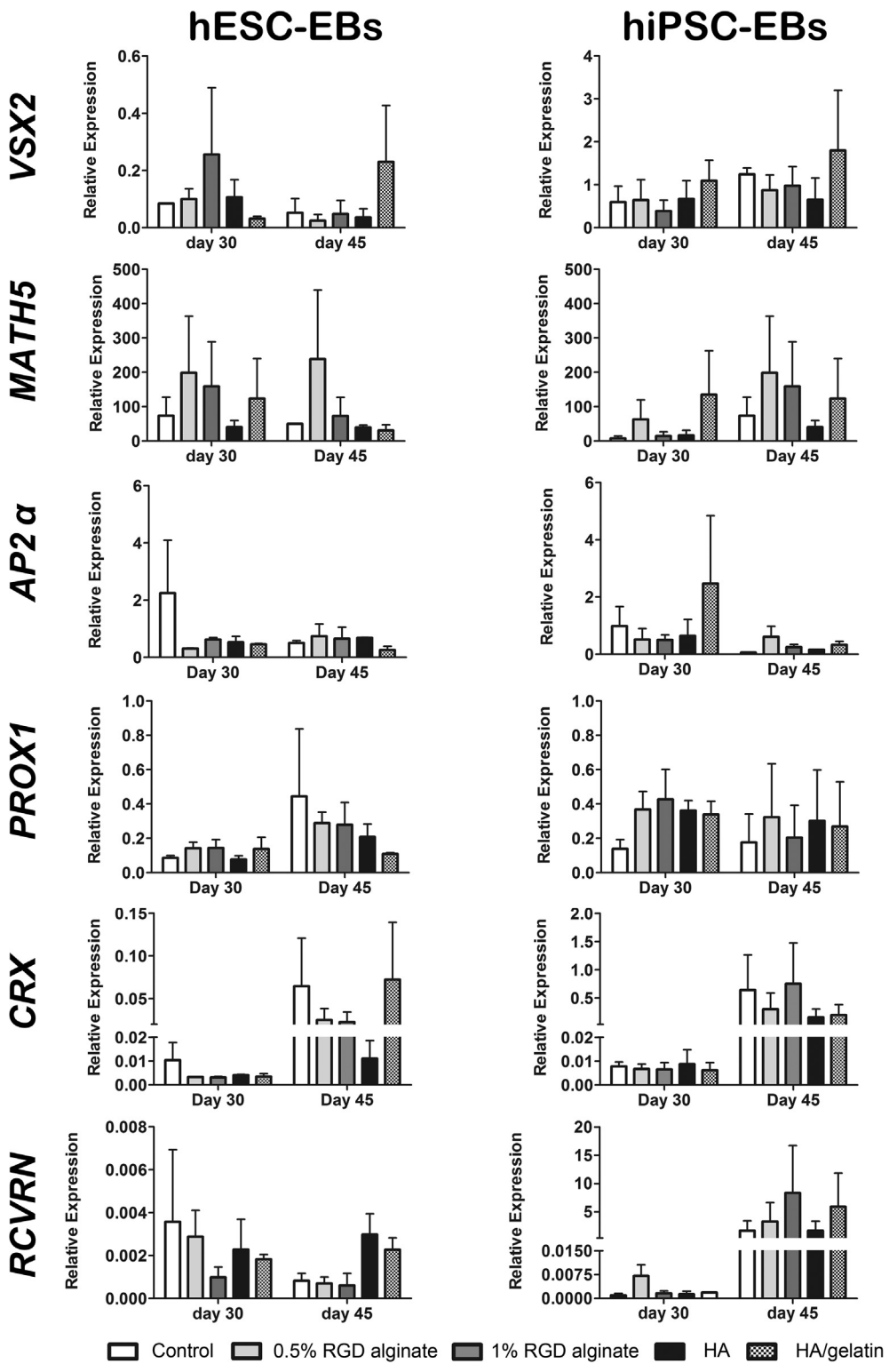

Fig. 6. The formation of neural retina is not adversely affected by hydrogel encapsulation. qRT-PCR analysis of neural retinal differentiation markers at days 30 and day 45 in hESC- and hiPSC-derived cultures as follows; *VSX2* (retinal progenitor cells); *MATH5* (retinal ganglion cells and their precursors); *AP2α* (amacrine cells and their precursors); *PROX1* (horizontal, amacrine and bipolar cell precursors and mature horizontal cells); *CRX* and *RECOVERIN* (photoreceptors and their precursors). 0.5% RGD-alginate increased the expression of the RGC marker, *MATH5* ($p < 0.05$). No other significant differences were observed between hydrogels and control conditions. This demonstrated that hydrogel encapsulation did not adversely affect formation and development of the neural retina, and may accelerate retinal ganglion cell production.

The apparent increase in retinal ganglion cell production along with RPE cells, which was observed in 0.5% RGD-alginate, may be due to the secretion of factors by RPE, such as pigment epithelium-derived factor (PEDF) by the RPE cells. RPE cells provide the majority of the PEDF which accumulates in the neural retina and has been proposed to be important for retinal ganglion cell development, regeneration and survival. Since retinal ganglion cells are the first neural retinal cells to arise [79], prolonged culture

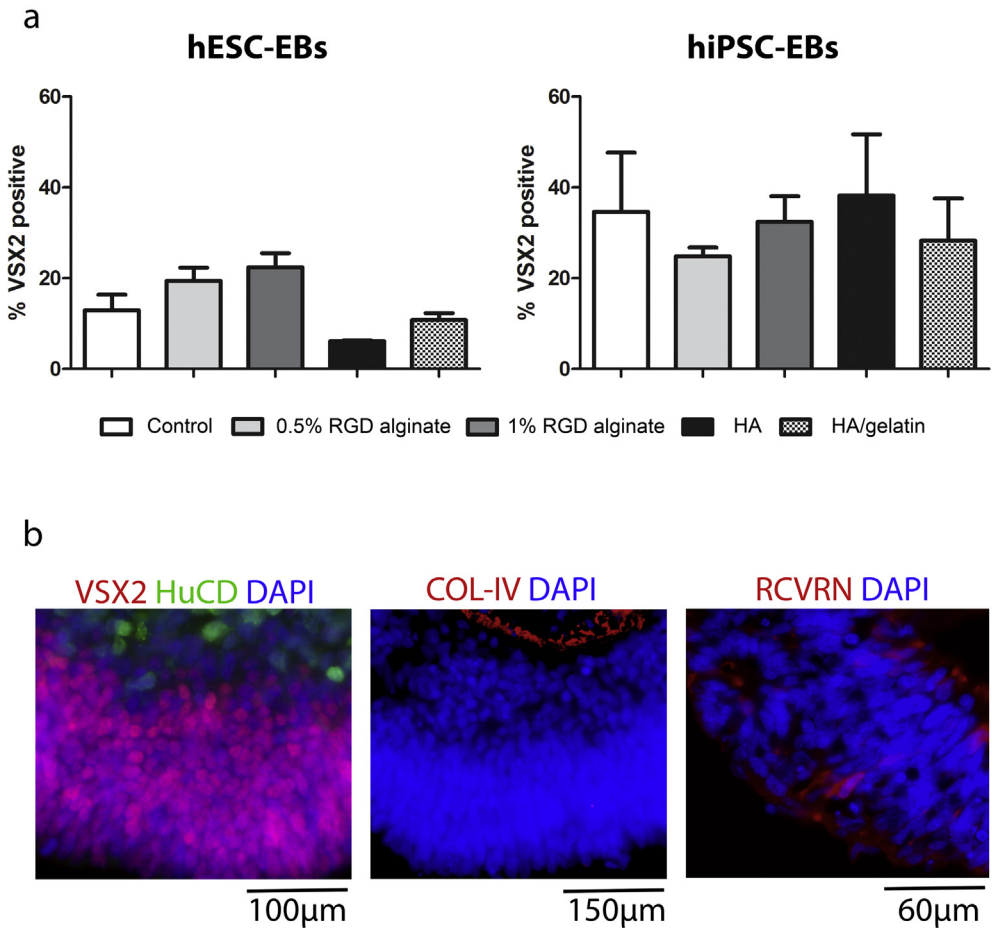

Fig. 7. The number of neural retinal progenitor cells was increased in 0.5% alginate hydrogel encapsulation. a) Flow cytometric analysis of VSX2-expressing cells at day 45 in hESC- and hiPSC-derived EBs was performed to compare the number of retinal progenitor cells under each condition. Encapsulation of EBs in different hydrogels had no significant effect on the number VSX2-positive cells ($p > 0.05$). This demonstrated that hydrogel encapsulation did not adversely affect retinal progenitor cell numbers, and confirmed the qRT-PCR analysis of *VSX2* expression shown in Fig. 7. b) Representative examples of IHC staining for VSX2 (retinal progenitor cells), HuCD (developing retinal ganglion cells and amacrine cells), RCVRN (photoreceptors and their precursors), and COL-IV at day 45. Similar staining was observed in all samples on days 30 and 45 and indicated that laminated neural retina was forming, as indicated by the qRT-PCR analysis shown in Fig. 7.

would be necessary to assess whether the derivation of other neural retinal cells, including photoreceptors, the development of which are also supported by the RPE [80–84], and further maturation of the laminated neural retina is also enhanced.

The mechanism by which the scaffold enhances retinal tissue formation is unclear. It was apparent from rheological characterisation that the mechanical properties are very different between the 0.5% RGD-alginate and the other three scaffolds, and the mechanical properties of the scaffold may, as has been shown with many other cells and tissues [67,85–91,43,92] play an important role in retinal differentiation. It is suggested that biomaterials with similar mechanical properties to the host tissue of interest can enhance differentiation towards the target lineages [67,89]. This occurs via mechano-transduction involving YAP/TAZ-mediated Hippo pathway signalling which ultimately leads to changes in the cytoskeleton, cell mechanics and chromatin condensation [86,93–95]. Limited data exist on the mechanical properties of retina [96–98], largely due to the fragility of the tissue and the limited thickness (approximated 0.25 mm) which makes such characterisation challenging. However, the elastic modulus of 0.5% RGD-alginate used in this study was found to be approximately 2 kPa, which is within the reported range of native mammalian retina, while the elastic modulus of 1% RGD-alginate, HA and HA/gelatin lay outside of the reported range [99]. This may, therefore, explain the most enhancing effects observed from EB encapsulation in 0.5% RGD-alginate hydrogel.

Additionally, cell-matrix (scaffold) binding, and therefore downstream signalling cascades resulting in differential cell behaviour [100–102], including cell differentiation [87], will also likely be markedly different between hydrogels. Cell-scaffold adhesion is mediated through the RGD motifs in RGD-alginate scaffolds (with the density being halved in 0.5% versus 1% RGD-alginate), which is bound by all five αV integrins, two β1 integrins (α5, α8) and αIIbβ3 [102]. In contrast, HA-binding is mediated by CD44 [103], CD168 (also known as RHAMM or HMMR) and layilin [104,105], while gelatin is proposed to be bound predominantly by the mannose receptor family [106] as well as RGD binding integrins [107,108].

Moreover, in the different hydrogels studied differential diffusion and accumulation of key proteins, including growth factors and ECM components, such as collagens, may occur [109,110]. This is likely due to the differences; in the net charge of the HA, gelatin, and RGD-alginate scaffolds; the apparent differences in pore sizes and interconnectivity [111]; and the differential presence of protein binding domain ligands, such as to the HA-binding domain in proteoglycans [112]. The differential accumulation of cell-synthesised ECM, the ultimate ECM-binding by the cells, and possible further differential accumulation of growth factors, will likely also influence differentiation [113,114]. Moreover, differences in the 3D surface topology of scaffolds have previously been reported to influence the differentiation of cells derived from hESCs [115] which may suggest the differences in pore wall smoothness and

pore sizes observed between scaffolds in this study may have influenced cell differentiation.

The present study may suggest that the use of RGD-alginate hydrogel is preferential to the HA-based hydrogels, which are currently being investigated for the delivery of retinal cells [44,49]. Furthermore, it provides a new approach for the enhanced generation of viable 3D laminated neural retina with simultaneous appearance of RPE foci which can be of useful significance for the derivation, transport and transplantation of this tissue into the compromised retina.

5. Conclusions

In this study it has been demonstrated that the derivation of RPE alone and in conjunction with neural retina from hESCs and hiPSCs is enhanced by culture in an RGD-alginate hydrogel scaffold. Further work should assess whether over a longer culture period the maturation of retinal tissue is enhanced, or whether additional optimisation of EB generation, in conjunction with this scaffold, can further improve retinal generation. Further work should seek to understand the mechanism of RGD-alginate scaffold-enhanced retinal ontogenesis. The findings may suggest that RGD-alginate could be preferential to HA-based hydrogels for *in vivo* delivery of retinal cells and this work may have implications for the derivation of other pigmented, neural or epithelial tissue.

Acknowledgments

We are grateful to Matthew Satterfield, Martin Kiening, Dr. Katarina Novakovik, Dr. Fernando Abegao, Katherine White and other members of the EM facility for SEM sample preparation and imaging assistance, and Dr. Andrew Filby and Gillian Hulme for assistance with FACS. We would like to thank members of our group for useful discussions and technical assistance, Pedram Panahi and Jonathan Kossoff for assistance with RPE quantification, and Jiajun Wang and Pengfei Duan for assistance with rheology. This work was funded by the ERC Consolidator award (#614620) and the RPFB Innovation award (#GR584) to ML. Author contributions were as follows: NH designed and performed research, data acquisition and analysis, and wrote the manuscript; DH performed research, data acquisition and analysis; AK performed data analysis; JC acquired and analysed data; CBM performed research and contributed to fundraising; DHWS performed research and contributed to fundraising; ML designed and performed research, manuscript writing and fundraising. All authors contributed to the final approval of manuscript.

Appendix A. Supplementary data

Supplementary data associated with this article can be found, in the online version, at http://dx.doi.org/10.1016/j.actbio.2016.11.016.

References

[1] G.A. Stevens, R.A. White, S.R. Flaxman, H. Price, J.B. Jonas, J. Keeffe, J. Leasher, K. Naidoo, K. Pesudovs, S. Resnikoff, H. Taylor, Global prevalence of vision impairment and blindness magnitude and temporal trends, E 2010, Ophthalmology 120 (2013) (1990) 2377–2384.
[2] D. Pascolini, S.P. Mariotti, Global estimates of visual impairment: 2010, Br. J. Ophthalmol. 96 (2012) 614–618.
[3] A. Lotery, X. Xu, G. Zlatava, J. Loftus, Burden of illness, visual impairment and health resource utilisation of patients with neovascular age-related macular degeneration: results from the UK cohort of a five-country cross-sectional study, Br. J. Ophthalmol. 91 (2007) 1303–1307.
[4] W.L. Wong, X. Su, X. Li, C.M.G. Cheung, R. Klein, C.-Y. Cheng, T.Y. Wong, Global prevalence of age-related macular degeneration and disease burden projection for 2020 and 2040: a systematic review and meta-analysis, Lancet Glob. Heal. 2 (2014) e106–e116.
[5] Q. Wang, J.H. Stern, S. Temple, Regenerative medicine: solution in sight, in: C. B. Rickman, M.M. LaVail, R.E. Anderson, C. Grimm, J. Hollyfield, J. Ash (Eds.), Retin. Degener. Dis., Springer, New York, 2016, pp. 543–548.
[6] N.D. Radtke, R.B. Aramant, H.M. Petry, P.T. Green, D.J. Pidwell, M.J. Seiler, Vision improvement in retinal degeneration patients by implantation of retina together with retinal pigment epithelium, Am. J. Ophthalmol. 146 (2008) 172–182.
[7] R.E. MacLaren, R.A. Pearson, A. MacNeil, R.H. Douglas, T.E. Salt, M. Akimoto, A. Swaroop, J.C. Sowden, R.R. Ali, Retinal repair by transplantation of photoreceptor precursors, Nature 444 (2006) 203–207.
[8] R.A. Pearson, A.C. Barber, M. Rizzi, C. Hippert, T. Xue, E.L. West, Y. Duran, A.J. Smith, J.Z. Chuang, S.A. Azam, U.F.O. Luhmann, A. Benucci, C.H. Sung, J.W. Bainbridge, M. Carandini, K.-W. Yau, J.C. Sowden, R.R. Ali, Restoration of vision after transplantation of photoreceptors, Nature 485 (2012) 99–103.
[9] K. Takahashi, K. Tanabe, M. Ohnuki, M. Narita, T. Ichisaka, K. Tomoda, Induction of pluripotent stem cells from adult human fibroblasts by defined factors, Cell 131 (2007) 861–872.
[10] F. Osakada, H. Ikeda, Y. Sasai, M. Takahashi, Stepwise differentiation of pluripotent stem cells into retinal cells, Nat. Protoc. 4 (2009) 811–824.
[11] R.H. Anderson, B. Chaudhry, T.J. Mohun, S.D. Bamforth, D. Hoyland, H.M. Phillips, S. Webb, A.F.M. Moorman, N.A. Brown, D.J. Henderson, Normal and abnormal development of the intrapericardial arterial trunks in humans and mice, Cardiovasc. Res. 95 (2012) 108–115.
[12] T. Nakano, S. Ando, N. Takata, M. Kawada, K. Muguruma, K. Sekiguchi, K. Saito, S. Yonemura, M. Eiraku, Y. Sasai, Self-formation of optic cups and storable stratified neural retina from human ESCs, Cell Stem Cell 10 (2012) 771–785.
[13] C.B. Mellough, J. Collin, M. Khazim, K. White, E. Sernagor, D.H.W. Steel, M. Lako, IGF-1 signaling plays an important role in the formation of three-dimensional laminated neural retina and other ocular structures from human embryonic stem cells, Stem Cells 33 (2015) 2416–2430.
[14] X. Zhong, C. Gutierrez, T. Xue, C. Hampton, M.N. Vergara, L.-H. Cao, A. Peters, T.S. Park, E.T. Zambidis, J.S. Meyer, D.M. Gamm, K.-W. Yau, M.V. Canto-Soler, Generation of three-dimensional retinal tissue with functional photoreceptors from human iPSCs, Nat. Commun. 5 (2014) 4047.
[15] H. Shirai, M. Mandai, Retinal regeneration by transplantation of retinal tissue derived from human embryonic or induced pluripotent stem cells, Inflamm. Regener. 36 (2016) 10–12.
[16] S.D. Schwartz, C.D. Regillo, B.L. Lam, D. Eliott, P.J. Rosenfeld, N.Z. Gregori, J. Hubschman, J.L. Davis, G. Heilwell, M. Spirn, J. Maguire, R. Gay, J. Bateman, R. M. Ostrick, D. Morris, M. Vincent, E. Anglade, L.V. Del Priore, Human embryonic stem cell-derived retinal pigment epithelium in patients with age-related macular degeneration and Stargardt ' s macular dystrophy : follow-up of two open-label phase 1/2 studies, Lancet 385 (2015) 509–516.
[17] C.B. Mellough, J. Collin, E. Sernagor, N.K. Wride, D.H.W. Steel, M. Lako, Lab generated retina: realizing the dream, Vis. Neurosci. (2014) 1–16.
[18] A. Daruich, A. Matet, F.-X. Borruat, Macular dystrophy associated with the mitochondrial DNA A3243G mutation: pericentral pigment deposits or atrophy? Report of two cases and review of the literature, BMC Ophthalmol. 14 (2014) 77.
[19] L.L. Leach, D.O. Clegg, Making stem cells retinal: methods for deriving retinal pigment epithelium and implications for patients with ocular disease, Stem Cells 33 (2015) 2363–2373.
[20] J. Reinhard, S.C. Joachim, A. Faissner, Extracellular matrix remodeling during retinal development, Exp. Eye Res. 133 (2015) 132–140.
[21] S.J. Clark, T.D.L. Keenan, H.L. Fielder, L.J. Collinson, R.J. Holley, C.L.R. Merry, T. H. van Kuppevelt, A.J. Day, P.N. Bishop, Mapping the differential distribution of glycosaminoglycans in the adult human retina, choroid, and sclera, Invest. Ophthalmol. Visual Sci. 52 (2011) 6511.
[22] M. Nasu, N. Takata, T. Danjo, H. Sakaguchi, T. Kadoshima, S. Futaki, K. Sekiguchi, M. Eiraku, Y. Sasai, Robust formation and maintenance of continuous stratified cortical neuroepithelium by laminin-containing matrix in mouse ES cell culture, PLoS One 7 (2012) 13–14.
[23] Y. Inoue, M. Yoneda, O. Miyaishi, M. Iwaki, M. Zako, Hyaluronan dynamics during retinal development, Brain Res. 1256 (2009) 55–60.
[24] J.G. Hollyfield, Hyaluronan and the functional organization of the interphotoreceptor matrix, Invest. Ophthalmol. Visual Sci. 40 (1999) 2767–2769.
[25] M. Ishikawa, Y. Sawada, T. Yoshitomi, Structure and function of the interphotoreceptor matrix surrounding retinal photoreceptor cells, Exp. Eye Res. 133 (2015) 3–18.
[26] M.R. Al-Ubaidi, M.I. Naash, S.M. Conley, A perspective on the role of the extracellular matrix in progressive retinal degenerative disorders, Invest. Ophthalmol. Visual Sci. 54 (2013) 8119.
[27] B. Kloeckener-Gruissem, J. Neidhardt, I. Magyar, H. Plauchu, J.-C. Zech, L. Morlé, S.M. Palmer-Smith, M.J. MacDonald, V. Nas, A.E. Fry, W. Berger, Novel VCAN mutations and evidence for unbalanced alternative splicing in the pathogenesis of Wagner syndrome, Eur. J. Hum. Genet. 352–356 (2012).
[28] G. Manes, I. Meunier, A. Avila-Fernandez, S. Banfi, G. Le Meur, X. Zanlonghi, M. Corton, F. Simonelli, P. Brabet, G. Labesse, I. Audo, S. Mohand-Said, C. Zeitz, J. A. Sahel, M. Weber, H. Dollfus, C.M. Dhaenens, D. Allorge, E. De Baere, R.K. Koenekoop, S. Kohl, F.P.M. Cremers, J.G. Hollyfield, A. Senechal, M. Hebrard, B. Bocquet, C.A. Garcia, C.P. Hamel, Mutations in IMPG1 cause vitelliform macular dystrophies, Am. J. Hum. Genet. 93 (2013) 571–578.

[29] D. Bandah-Rozenfeld, R.W.J. Collin, E. Banin, L. Ingeborgh Van Den Born, K.L. M. Coene, A.M. Siemiatkowska, L. Zelinger, M.I. Khan, D.J. Lefeber, I. Erdinest, F. Testa, F. Simonelli, K. Voesenek, E.A.W. Blokland, T.M. Strom, C.C.W. Klaver, R. Qamar, S. Banfi, F.P.M. Cremers, D. Sharon, A.I. Den Hollander, Mutations in IMPG2, encoding interphotoreceptor matrix proteoglycan 2, cause autosomal-recessive retinitis pigmentosa, Am. J. Hum. Genet. 87 (2010) 199–208.
[30] R. Ratnapriya, X. Zhan, R.N. Fariss, K.E. Branham, D. Zipprer, C.F. Chakarova, Y. V. Sergeev, M.M. Campos, M. Othman, J.S. Friedman, A. Maminishkis, N.H. Waseem, M. Brooks, H.K. Rajasimha, A.O. Edwards, A. Lotery, B.E. Klein, B.J. Truitt, B. Li, D.A. Schaumberg, D.J. Morgan, M.A. Morrison, E. Souied, E.E. Tsironi, F. Grassmann, G.A. Fishman, G. Silvestri, H.P.N. Scholl, I.K. Kim, J. Ramke, J. Tuo, J.E. Merriam, J.C. Merriam, K.H. Park, L.M. Olson, L.A. Farrer, M. P. Johnson, N.S. Peachey, M. Lathrop, R.V. Baron, R.P. Igo, R. Klein, S.A. Hagstrom, Y. Kamatani, T.M. Martin, Y. Jiang, Y. Conley, J.A. Sahel, D.J. Zack, C. C. Chan, M.A. Pericak-Vance, S.G. Jacobson, M.B. Gorin, M.L. Klein, R. Allikmets, S.K. Iyengar, B.H. Weber, J.L. Haines, T. Léveillard, M.M. Deangelis, D. Stambolian, D.E. Weeks, S.S. Bhattacharya, E.Y. Chew, J.R. Heckenlively, G.R. Abecasis, A. Swaroop, Rare and common variants in extracellular matrix gene Fibrillin 2 (FBN2) are associated with macular degeneration, Hum. Mol. Genet. 23 (2014) 5827–5837.
[31] H. Nakazato, S. Hattori, T. Matsuura, Y. Koitabashi, F. Endo, I. Matsuda, Identification of a single base insertion in the COL4A5 gene in Alport syndrome, Kidney Int. 44 (1993) 1091–1096.
[32] J. Savige, J. Liu, D.C. DeBuc, J.T. Handa, G.S. Hageman, Y.Y. Wang, J.D. Parkin, B. Vote, R. Fassett, S. Sarks, D. Colville, Retinal basement membrane abnormalities and the retinopathy of Alport syndrome, Invest. Ophthalmol. Visual Sci. 51 (2010) 1621–1627.
[33] A.L. Sertié, V. Sossi, A.A. Camargo, M. Zatz, C. Brahe, M.R. Passos-Bueno, Collagen XVIII, containing an endogenous inhibitor of angiogenesis and tumor growth, plays a critical role in the maintenance of retinal structure and in neural tube closure (Knobloch syndrome), Hum. Mol. Genet. 9 (2000) 2051–2058.
[34] G. Pinzón-Duarte, G. Daly, Y.N. Li, M. Koch, W.J. Brunken, Defective formation of the inner limiting membrane in laminin β2- and β3-null mice produces retinal dysplasia, Invest. Ophthalmol. Visual Sci. 51 (2010) 1773–1782.
[35] P.J. Uren, J.T. Lee, M.M. Doroudchi, A.D. Smith, A. Horsager, A profile of transcriptomic changes in the rd10 mouse model of retinitis pigmentosa, Mol. Visual 20 (2014) 1612–1628.
[36] J.M. Gross, B.D. Perkins, A. Amsterdam, A. Egana, T. Darland, J.I. Matsui, S. Sciascia, N. Hopkins, J.E. Dowling, Identification of Zebrafish insertional mutants with defects in visual system development and function, Genetics 170 (2005) 245–261.
[37] L. Fu, D. Garland, Z. Yang, D. Shukla, A. Rajendran, E. Pearson, E.M. Stone, K. Zhang, E.A. Pierce, The R345W mutation in EFEMP1 is pathogenic and causes AMD-like deposits in mice, Hum. Mol. Genet. 16 (2007) 2411–2422.
[38] C.A. May, Distribution of nidogen in the murine eye and ocular phenotype of the nidogen-1 knockout mouse, ISRN Ophthalmol. 2012 (2012) 378641.
[39] R.A. Pearson, Advances in repairing the degenerate retina by rod photoreceptor transplantation, Biotechnol. Adv. 32 (2014) 485–491.
[40] T.D.L. Keenan, S.J. Clark, R.D. Unwin, L.A. Ridge, A.J. Day, P.N. Bishop, Mapping the differential distribution of proteoglycan core proteins in the adult human retina, choroid, and sclera, Invest. Ophthalmol. Visual Sci. 53 (2012) 7528–7538.
[41] S. Acharya, V.C. Foletta, J.W. Lee, M.E. Rayborn, I.R. Rodriguez, W.S. Young, J.G. Hollyfield, SPACRCAN, a novel human interphotoreceptor matrix hyaluronan-binding proteoglycan synthesized by photoreceptors and pinealocytes, J. Biol. Chem. 275 (2000) 6945–6955.
[42] P deS Senanayake, A. Calabro, K. Nishiyama, J.G. Hu, D. Bok, J.G. Hollyfield, Glycosaminoglycan synthesis and secretion by the retinal pigment epithelium: polarized delivery of hyaluronan from the apical surface, J. Cell Sci. 114 (2001) 199–205.
[43] S.K. Seidlits, Z.Z. Khaing, R.R. Petersen, J.D. Nickels, J.E. Vanscoy, J.B. Shear, C.E. Schmidt, The effects of hyaluronic acid hydrogels with tunable mechanical properties on neural progenitor cell differentiation, Biomaterials 31 (2010) 3930–3940.
[44] B.G. Ballios, M.J. Cooke, D. van der Kooy, M.S. Shoichet, A hydrogel-based stem cell delivery system to treat retinal degenerative diseases, Biomaterials 31 (2010) 2555–2564.
[45] Y. Liu, R. Wang, T.I. Zarembinski, N. Doty, C. Jiang, C. Regatieri, X. Zhang, M.J. Young, The application of hyaluronic acid hydrogels to retinal progenitor cell transplantation, Tissue Eng. Part A 19 (2012) 135–142.
[46] T.I. Zarembinski, N.J. Doty, I.E. Erickson, R. Srinivas, B.M. Wirostko, W.P. Tew, Thiolated hyaluronan-based hydrogels crosslinked using oxidized glutathione: an injectable matrix designed for ophthalmic applications, Acta Biomater. 10 (2014) 94–103.
[47] M.A.J. Mazumder, S.D. Fitzpatrick, B. Muirhead, H. Sheardown, Cell-adhesive thermogelling PNIPAAm/hyaluronic acid cell delivery hydrogels for potential application as minimally invasive retinal therapeutics, J. Biomed. Mater. Res. A 100 (2012) 1877–1887.
[48] Y. Aizawa, M.S. Shoichet, The role of endothelial cells in the retinal stem and progenitor cell niche within a 3D engineered hydrogel matrix, Biomaterials 33 (2012) 5198–5205.
[49] B.G. Ballios, M.J. Cooke, L. Donaldson, B.L.K. Coles, C.M. Morshead, D. van der Kooy, M.S. Shoichet, A hyaluronan-based injectable hydrogel improves the survival and integration of stem cell progeny following transplantation, Stem Cell Rep. 4 (2015) 1031–1045.
[50] T.-W. Wang, M. Spector, Development of hyaluronic acid-based scaffolds for brain tissue engineering, Acta Biomater. 5 (2009) 2371–2384.
[51] R. Aramant, Transplanted Sheets of Human Retina and Retinal Pigment Epithelium Develop Normally in Nude Rats, Exp. Eye Res. 75 (2002) 115–125.
[52] L. Li, A.E. Davidovich, J.M. Schloss, U. Chippada, R.R. Schloss, L.A. Langrana, M. L. Yarmush, Neural lineage differentiation of embryonic stem cells within alginate microbeads, Biomaterials 32 (2011) 4489–4497.
[53] J. Wikstrom, M. Elomaa, H. Syvajarvi, J. Kuokkanen, M. Yliperttula, P. Honkakoski, A. Urtti, Alginate-based microencapsulation of retinal pigment epithelial cell line for cell therapy, Biomaterials 29 (2008) 869–876.
[54] R. Heidari, Z.-S. Soheili, S. Samiei, H. Ahmadieh, M. Davari, F. Nazemroaya, A. Bagheri, A. Deezagi, Alginate as a cell culture substrate for growth and differentiation of human retinal pigment epithelial cells, Appl. Biochem. Biotechnol. 175 (2015) 2399–2412.
[55] T.E. Eurell, D.R. Brown, P.A. Gerding, R.E. Hamor, Alginate as a new biomaterial for the growth of porcine retinal pigment epithelium, Vet. Ophthalmol. 6 (2003) 237–243.
[56] M.J. Rah, A review of hyaluronan and its ophthalmic applications, Optometry 82 (2011) 38–43.
[57] C. Schramm, M.S. Spitzer, S. Henke-Fahle, G. Steinmetz, K. Januschowski, P. Heiduschka, J. Geis-Gerstorfer, T. Biedermann, K.U. Bartz-Schmidt, P. Szurman, The cross-linked biopolymer hyaluronic acid as an artificial vitreous substitute, Invest. Ophthalmol. Visual Sci. 53 (2012) 613–621.
[58] N.C. Hunt, L.M. Grover, Encapsulation and culture of mammalian cells including corneal cells in alginate hydrogels, in: B. Wright, C.J. Connon (Eds.), Corneal Regen., Humana Press, New York, Med., 2013, pp. 201–210.
[59] M. Caiazzo, Y. Okawa, A. Ranga, A. Piersigilli, Y. Tabata, M.P. Lutolf, Defined three-dimensional microenvironments boost induction of pluripotency, Nat. Mater. 15 (2016).
[60] A. Kunitomi, S. Yuasa, F. Sugiyama, Y. Saito, T. Seki, D. Kusumoto, S. Kashimura, M. Takei, S. Tohyama, H. Hashimoto, T. Egashira, Y. Tanimoto, S. Mizuno, S. Tanaka, H. Okuno, K. Yamazawa, H. Watanabe, M. Oda, R. Kaneda, Y. Matsuzaki, T. Nagai, H. Okano, K. Yagami, M. Tanaka, H1foo has a pivotal role in qualifying induced pluripotent stem cells, Stem Cell Rep. 6 (2016) 1–9.
[61] G. Liang, Y. Zhang, Genetic and epigenetic variations in iPSCs: Potential causes and implications for application, Cell Stem Cell 13 (2013) 149–159.
[62] L. Leach, R. Croze, Q. Hu, V. Nadar, T. Clevenger, B. Pennington, D. Gamm, D. Clegg, Induced pluripotent stem cell-derived retinal pigmented epithelium: a comparative study between cell lines and differentiation methods, J. Ocul. Pharmacol. Ther. 32 (2016) 1–14.
[63] D. Hiler, X. Chen, J. Hazen, S. Kupriyanov, P.A. Carroll, C. Qu, B. Xu, D. Johnson, L. Griffiths, S. Frase, A.R. Rodriguez, G. Martin, J. Zhang, J. Jeon, Y. Fan, D. Finkelstein, R.N. Eisenman, K. Baldwin, M.A. Dyer, Quantification of Retinogenesis in 3D Cultures Reveals Epigenetic Memory and Higher Efficiency in iPSCs Derived from Rod Photoreceptors, Cell Stem Cell 17 (2015) 101–115.
[64] B.B. Thomas, D. Zhu, L. Zhang, P.B. Thomas, Y. Hu, H. Nazari, F. Stefanini, P. Falabella, D.O. Clegg, D.R. Hinton, M.S. Humayun, Survival and functionality of hESC-derived retinal pigment epithelium cells cultured as a monolayer on polymer substrates transplanted in RCS rats, Invest. Opthalmol Visual Sci. 57 (2016) 2877.
[65] Q. Hu, A.M. Friedrich, L.V. Johnson, D.O. Clegg, Memory in induced pluripotent stem cells: reprogrammed human retinal-pigmented epithelial cells show tendency for spontaneous redifferentiation, Stem Cells 28 (2010) 1981–1991.
[66] M. White, D. Srivastava, Limited gene expression variation in human embryonic stem cell and induced pluripotent stem cell derived endothelial cells, Stem Cells 31 (2013) 92–103.
[67] A.J. Keung, P. Asuri, S. Kumar, D.V. Schaffer, Soft microenvironments promote the early neurogenic differentiation but not self-renewal of human pluripotent stem cells, Integr. Biol. 4 (2012) 1049–1058.
[68] H. Suga, T. Kadoshima, M. Minaguchi, M. Ohgushi, M. Soen, T. Nakano, N. Takata, T. Wataya, K. Muguruma, H. Miyoshi, S. Yonemura, Y. Oiso, Y. Sasai, Self-formation of functional adenohypophysis in three-dimensional culture, Nature 480 (2011) 57–62.
[69] M. Eiraku, N. Takata, H. Ishibashi, M. Kawada, E. Sakakura, S. Okuda, K. Sekiguchi, T. Adachi, Y. Sasai, Self-organizing optic-cup morphogenesis in three-dimensional culture, Nature 472 (2011) 51–56.
[70] M. Eiraku, K. Watanabe, M. Matsuo-Takasaki, M. Kawada, S. Yonemura, M. Matsumura, T. Wataya, A. Nishiyama, K. Muguruma, Y. Sasai, Self-organized formation of polarized cortical tissues from ESCS and its active manipulation by extrinsic signals, Cell Stem Cell 3 (2008) 519–532.
[71] X. Zhong, C. Gutierrez, T. Xue, C. Hampton, M. Natalia, L. Cao, A. Peters, T. Park, E.T. Zambidis, J.S. Meyer, D.M. Gamm, K. Yau, M.V. Canto-soler, Generation of three dimensional retinal tissue with functional photoreceptors from human iPSCs, Nat. Commun. 5 (2015) 1–31.
[72] M. Parvini, K. Parivar, F. Safari, M. Tondar, Generation of eye field/optic vesicle-like structures from human embryonic stem cells under two-dimensional and chemically defined conditions, Vitr. Cell. Dev. Biol. Anim. 51 (2015) 310–318.
[73] B.A. Tucker, R.F. Mullins, L.M. Streb, K. Anfnson, M.E. Eyestone, E. Kaalberg, M. J. Riker, A.V. Drack, T.A. Braun, E.M. Stone, Patient-specifc iPSC-derived photoreceptor precursor cells as a means to investigate retinitis pigmentosa, Elife 2013 (2013) 1–18.

[74] D. Lukovic, A. Artero Castro, A.B.G. Delgado, M. de, L.A.M. Bernal, N. Luna Pelaez, A. Díez Lloret, R. Perez Espejo, K. Kamenarova, L. Fernández Sánchez, N. Cuenca, M. Cortón, A. Avila Fernandez, A. Sorkio, H. Skottman, C. Ayuso, S. Erceg, S.S. Bhattacharya, Human iPSC derived disease model of MERTK-associated retinitis pigmentosa, Sci. Rep. 5 (2015) 12910.
[75] Z. Ablonczy, M. Dahrouj, P.H. Tang, Y. Liu, K. Sambamurti, A.D. Marmorstein, C.E. Crosson, Human retinal pigment epithelium cells as functional models for the RPE in vivo, Invest. Ophthalmol. Visual Sci. 52 (2011) 8614–8620.
[76] A. Maminishkis, S. Chen, S. Jalickee, T. Banzon, G. Shi, F.E. Wang, T. Ehalt, J.A. Hammer, S.S. Miller, Confluent monolayers of cultured human fetal retinal pigment epithelium exhibit morphology and physiology of native tissue 47 (2006) 3612–3624.
[77] A.V. Kuznetsova, A.M. Kurinov, M.A. Aleksandrova, A.V. Kuznetsova, A.M. Kurinov, M.A. Aleksandrova, Cell models to study regulation of cell transformation in pathologies of retinal pigment epithelium, J. Ophthalmol. 2014 (2014) 1–18.
[78] J. Tian, K. Ishibashi, S. Honda, S.A. Boylan, L.M. Hjelmeland, J.T. Handa, The expression of native and cultured human retinal pigment epithelial cells grown in different culture conditions, Br. J. Ophthalmol. 89 (2005) 1510–1517.
[79] M. Hoon, H. Okawa, L. Della Santina, R.O.L. Wong, Functional architecture of the retina: development and disease, Prog. Retin. Eye Res. 42 (2014) 44–84.
[80] O.L. German, E. Buzzi, N.P. Rotstein, E. Rodríguez-Boulan, L.E. Politi, Retinal pigment epithelial cells promote spatial reorganization and differentiation of retina photoreceptors, J. Neurosci. Res. 86 (2008) 3503–3514.
[81] S.P. Becerra, R.N. Fariss, Y.Q. Wu, L.M. Montuenga, P. Wong, B.A. Pfeffer, Pigment epithelium-derived factor in the monkey retinal pigment epithelium and interphotoreceptor matrix: apical secretion and distribution, Exp. Eye Res. 78 (2004) 223–234.
[82] S. Patricia, Becerra, focus on molecules: pigment epithelium-derived factor (PEDF), Exp. Eye Res. 82 (2006) 739–740.
[83] C.J. Barnstable, J. Tombran-Tink, Neuroprotective and antiangiogenic actions of PEDF in the eye: Molecular targets and therapeutic potential, Prog. Retin. Eye Res. 23 (2004) 561–577.
[84] V. Vigneswara, M. Esmaeili, L. Deer, M. Berry, A. Logan, Z. Ahmed, Eye drop delivery of pigment epithelium-derived factor-34 promotes retinal ganglion cell neuroprotection and axon regeneration, Mol. Cell. Neurosci. 68 (2015) 212–221.
[85] S. Gobaa, S. Hoehnel, M.P. Lutolf, Substrate elasticity modulates the responsiveness of mesenchymal stem cells to commitment cues, Integr. Biol. (Camb) 7 (2015) 1135–1142.
[86] Y. Shao, J. Sang, J. Fu, On human pluripotent stem cell control: The rise of 3D bioengineering and mechanobiology, Biomaterials 52 (2015) 26–43.
[87] J. Lee, A.A. Abdeen, X. Tang, T.A. Saif, K.A. Kilian, Geometric guidance of integrin mediated traction stress during stem cell differentiation, Biomaterials 69 (2015) 174–183.
[88] E. Bellas, C.S. Chen, Forms, forces, and stem cell fate, Curr. Opin. Cell Biol. 31 (2014) 92–97.
[89] A.J. Engler, S. Sen, H.L. Sweeney, D.E. Discher, Matrix elasticity directs stem cell lineage specification, Cell 126 (2006) 677–689.
[90] W.L. Murphy, T.C. McDevitt, A.J. Engler, Materials as stem cell regulators, Nat. Mater. 13 (2014) 547–557.
[91] K. Saha, A.J. Keung, E.F. Irwin, Y. Li, L. Little, D.V. Schaffer, K.E. Healy, Substrate modulus directs neural stem cell behavior, Biophys. J. 95 (2008) 4426–4438.
[92] J.-W. Shin, D.J. Mooney, Improving stem cell therapeutics with mechanobiology, Cell Stem Cell 18 (2016) 16–19.
[93] F.-M. Chen, X. Liu, Advancing Biomaterials of Human Origin for Tissue Engineering, Prog. Polym. Sci. (2015).
[94] J. Chen, J. Irianto, S. Inamdar, P. Pravincumar, D.A. Lee, D.L. Bader, M.M. Knight, Cell mechanics, structure, and function are regulated by the stiffness of the three-dimensional microenvironment, Biophys. J. 103 (2012) 1188–1197.
[95] G. Halder, S. Dupont, S. Piccolo, Transduction of mechanical and cytoskeletal cues by YAP and TAZ, Nat. Rev. Mol. Cell Biol. 13 (2012) 591–600.
[96] K. Chen, A.P. Rowley, J.D. Weiland, M.S. Humayun, Elastic properties of human posterior eye, J. Biomed. Mater. Res. Part A 102 (2014) 2001–2007.
[97] K.S. Worthington, L.A. Wiley, A.M. Bartlett, E.M. Stone, R.F. Mullins, A.K. Salem, C.A. Guymon, B.A. Tucker, Mechanical properties of murine and porcine ocular tissues in compression, Exp. Eye Res. 121 (2014) 194–199.
[98] P.B. Henrich, L.A. Gurski, S. Pradhan-Bhatt, R.L. Witt, M.C. Farach-Carson, X. Jia, Nanoscale topographic and biomechanical studies of the human internal limiting membrane, Invest. Ophthalmol. Visual Sci. 53 (2012) 2561–2570.
[99] K. Franze, M. Francke, K. Günter, A.F. Christ, N. Körber, A. Reichenbach, J. Guck, Spatial mapping of the mechanical properties of the living retina using scanning force microscopy, Soft Matter 7 (2011) 3147–3154.
[100] E. Hohenester, Signalling complexes at the cell-matrix interface, Curr. Opin. Struct. Biol. 29 (2014) 10–16.
[101] R.O. Hynes, Integrins : bidirectional, allosteric signaling machines in their roles as major adhesion receptors, integrins, Cell 110 (2002) 673–687.
[102] J.D. Humphries, A. Byron, M.J. Humphries, humphries intergrin biding pic.pdf, 2006.
[103] S. Goodison, V. Urquidi, D. Tarin, CD44 cell adhesion molecules, Mol. Pathol. 52 (1999) 189–196.
[104] R. Frischknecht, C.I. Seidenbecher, The crosstalk of hyaluronan-based extracellular matrix and synapses, Neuron Glia Biol. 4 (2008) 249.
[105] R.E. Hausman, Ocular extracellular matrices in development, Prog. Retin. Eye Res. 26 (2007) 162–188.
[106] B. Leitinger, E. Hohenester, Mammalian collagen receptors, Matrix Biol. 26 (2007) 146–155.
[107] A.V. Taubenberger, M.A. Woodruff, H. Bai, D.J. Muller, D.W. Hutmacher, The effect of unlocking RGD-motifs in collagen I on pre-osteoblast adhesion and differentiation, Biomaterials 31 (2010) 2827–2835.
[108] M. Yamamoto, M. Yamato, M. Aoyagi, K. Yamamoto, Identification of integrins involved in cell adhesion to native and denatured type I collagens and the phenotypic transition of rabbit arterial smooth muscle cells, Exp Cell Res. 219 (1995) 249–256.
[109] A.M. Smith, N.C. Hunt, R.M. Shelton, G. Birdi, L.M. Grover, Alginate hydrogel has a negative impact on in vitro collagen 1 deposition by fibroblasts, Biomacromolecules 13 (2012) 4032–4038.
[110] S. Kirchhof, A.M. Goepferich, F.P. Brandl, Hydrogels in Ophthalmic Applications, Eur. J. Pharm. Biopharm. (2015).
[111] R. Censi, P. Di Martino, T. Vermonden, W.E. Hennink, Hydrogels for protein delivery in tissue engineering, J. Control. Release 161 (2012) 680–692.
[112] K.T. Dicker, L.A. Gurski, S. Pradhan-Bhatt, R.L. Witt, M.C. Farach-Carson, X. Jia, Hyaluronan: a simple polysaccharide with diverse biological functions, Acta Biomater. 10 (2014) 1558–1570.
[113] R.J. Holley, K.A. Meade, C.L.R. Merry, Using embryonic stem cells to understand how glycosaminoglycans regulate differentiation, Biochem. Soc. Trans. 42 (2014) 689–695.
[114] K. Forsten-Williams, C.L. Chu, M. Fannon, J.A. Buczek-thomas, M.A. Nugent, Control of growth factor networks by heparan sulfate proteoglycans, Annu. Rev. Biomed. Eng. 36 (2008) 2134–2148.
[115] P. Viswanathan, M.G. Ondeck, S. Chirasatitsin, K. Ngamkham, G.C. Reilly, A.J. Engler, G. Battaglia, 3D surface topology guides stem cell adhesion and differentiation, Biomaterials 52 (2015) 140–147.